THE UNIVERSITY OF MICHIGAN
ANN ARBOR, MICHIGAN

QUARTERLY PROGRESS REPORT NO. 10

ON

BASIC RESEARCH IN MICROWAVE DEVICES AND QUANTUM ELECTRONICS

This report covers the period August 1, 1965 to December 1, 1965

Electron Physics Laboratory
Department of Electrical Engineering

By: B. Ho
N. A. Masnari
J. E. Rowe
C. Yeh

Approved by: C. Yeh
Project Engineer

Approved by: J. E. Rowe
J. E. Rowe, Director
Electron Physics Laboratory

Project 05772

DEPARTMENT OF THE NAVY
BUREAU OF SHIPS
WASHINGTON 25, D.C.
PROJECT SERIAL NO. SR0080301, TASK 9391
CONTRACT NO. NObsr-89274

December, 1965

Eugu
LMR
Ø567

ABSTRACT

The problems of beam expansion and phase focusing in the case of cyclotron-cyclotron and cyclotron-synchronous wave interactions in a d-c pumped quadrupole amplifier are studied and compared. Although it seems that cyclotron-cyclotron wave interaction is more favorable compared to cyclotron-synchronous wave interaction as far as beam expansion is concerned, the phase focusing in the latter case is so strong that the beam never has time to expand before it is brought back into focus again.

A theoretical computation of the cross-modulation products in a wideband tunnel-diode amplifier with two input signals of slightly different frequencies has been made. The effect on the output products of varying the relative amplitudes of the input signals is shown in a series of graphs.

Results on the experimental measurements of the cross-modulation products of a Crestatron power amplifier with two input signals of slightly different frequencies are shown in detail. These results indicate that the $2f_1$ and $2f_2$ harmonics are the strongest modulation products if they happen to be within the bandwidth of the amplifier. Otherwise, the components $2f_1-f_2$ or $2f_2-f_1$ will be the stronger. The effect on the output products of varying the relative power level of the input signals has been investigated in great detail.

TABLE OF CONTENTS

LIST OF ILLUSTRATIONS

PERSONNEL

Scientific and Engineering Personnel		Time Worked in Man Months*
J. Rowe	Professors of Electrical Engineering	.20
C. Yeh		1.51
D. Solomon	Associate Research Engineer	.39
W. Bond	Associate Research Mathematician	1.36
B. Ho	Research Associate	.62
A. Cha	Assistant in Research	1.51
Service Personnel		6.16

* Time Worked is based on 172 hours per month.

ARTICLE ISSUED DURING THE LAST QUARTER

C. Yeh and B. Ho, "Electron Trajectories and Energy Relations in Transverse-Wave Amplifiers", Proc. IEEE, (Letter to Editor), vol. 53, No. 9, pp. 1242-1244; September, 1965.

QUARTERLY PROGRESS REPORT NO. 10

ON

BASIC RESEARCH IN MICROWAVE DEVICES AND QUANTUM ELECTRONICS

1. General Introduction (C. Yeh)

The broad purpose of this project is to investigate new ideas in the area of microwave devices and quantum electronics. The program is envisioned as a general and flexible one under which a wide variety of topics may be studied. At present, the following areas of investigation are in progress:

A. Study of frequency multiplication in an angular propagating structure. Redesigning of a low-frequency multiplier tube which multiplies a 600-mc input signal to a 2400-mc output signal with adjustable feedback control is in progress and the tube has been assembled and will soon be ready for processing.

B. Study of a d-c pumped quadrupole amplifier. Before proceeding to design a d-c pumped quadrupole amplifier, other phases of the theoretical analysis will be performed. These include the problems of beam expansion and phase focusing. Cyclotron-synchronous wave interaction is compared to cyclotron-cyclotron wave interaction in these respects.

C. Investigation of the cross-modulation products in a wideband tunnel-diode amplifier. The previously derived expression for the V-I characteristic of a tunnel diode is used to compute the cross-modulation products at the output of the amplifier when the input consists of two input signals at slightly different frequencies. The effect of varying the ratio of the amplitudes of input signals on the modulation products at the output will also be studied.

D. Multisignal Crestatron operation. The experimental determination of the cross-modulation products of a traveling-wave amplifier with multiple-signal inputs is extended to cover the Crestatron mode of operation. Starting with two input signals, the effect of the relative power levels of the input signals on the cross-modulation products of the output is measured. Further extension of the experiments to three input signals and a band of noise as an input is planned.

E. Theoretical studies on multisignal microwave amplifiers. Nonlinear calculations are being carried out for the cross-modulation products of O- and M-type amplifiers as a continuation of the theoretical study initiated earlier. A nonlinear theory of a crossed-field injected-beam amplifier with multisignal input will be developed along the same line.

2. Study of Frequency Multiplication in an Angular Propagating Circuit

Supervisor: C. Yeh

Staff: B. Ho

The redesigned tube is now in the final stages of assembly. A beam trimmer is being added in order to trim the beam diameter down to approximately 0.5 mm. The cold test on the multiple cavity and the three Cuccia couplers has been completed. The tube will be tested as soon as it is ready.

3. Study of a D-c Pumped Quadrupole Amplifier

Supervisor: C. Yeh

Staff: B. Ho

3.1 Introduction. Computer solutions of the trajectories of electrons reveal more interesting results. Two of these results will be discussed in this report. These are the problems of beam expansion and phase focusing. The former is due to the fact that different parts

of the electron beam react differently to the pump field in the pump structure and some of the electrons may grow in orbital radius and eventually be intercepted by the structure. The latter is an automatic sorting mechanism which brings more electrons to work in favor of amplification.

3.2 The Effect of Beam Expansion. When a finite electron beam passes through the quadrupole pump field structure, electrons from different locations of the beam will react differently with the pump field. Consequently, some of the electrons will grow in orbit and intercept the pump structure. This beam expansion phenomenon is unavoidable in all transverse-wave amplifiers. The effect becomes more serious when the physical size of the beam is comparable to the size of the pump field structure. When the physical size of the beam is large, early beam interception will limit the possibility of high-gain operation. The amount of beam expansion for individual electrons is very sensitive to their locations with respect to the pump field structure.

The beam expansion effects in the quadrifilar helix pump field for a finite beam for both cyclotron-cyclotron and cyclotron-synchronous wave interactions can be studied through the use of the equations of motion derived in Quarterly Progress Reports No. 5 and No. 6. For an unmodulated finite-diameter beam entering the structure, the initial condition, $d\theta/dt = 0$ at $t = 0$, is used. In rotational coordinates this initial condition becomes

$$\left.\frac{d\Phi}{d\tau}\right|_o = -1 \quad .$$

The trajectories of electrons in response to certain pump field configurations are computed. Since the electrons on the circumference

of the beam are affected most, only those electrons are considered in the analysis. Assume that the beam has a radius of $\rho_o = 0.1$. Four angular locations, $\Phi_o = 0$, 45, 90 and 135 degrees, for each pump field strength are used in the computation.

The computer solutions of beam expansion effects for cyclotron-cyclotron wave interaction with different pump field strengths are shown in Figs. 3.1 through 3.3. For cyclotron-synchronous wave interaction, the results are shown in Figs. 3.4 through 3.7.

From these computer solutions, several points are observed:

1. The beam expansion phenomenon is more pronounced in the case of cyclotron-synchronous wave interaction.

2. The amount of beam expansion is directly proportional to the pump field strength.

3. The least expanded electrons are those located at $\Phi = 0$ degrees, while those most affected are located 90 degrees from the least expanded ones.

It can be concluded from these observations that for cyclotron-cyclotron wave interaction the beam expansion is less important than in the case of cyclotron-synchronous wave interaction. For a medium strength pump field, as shown in Fig. 3.2 for cyclotron-cyclotron wave interaction, the beam remains reasonably well focused. In the case of cyclotron-synchronous wave interaction, the beam expansion is more pronounced and even for a medium strength pump field, as shown in Fig. 3.6, the beam diverges gradually. However, the actual situation is not as bad as it appears due to the phase-focusing effect to be discussed later. The beam will actually shift back to the most favorable phase

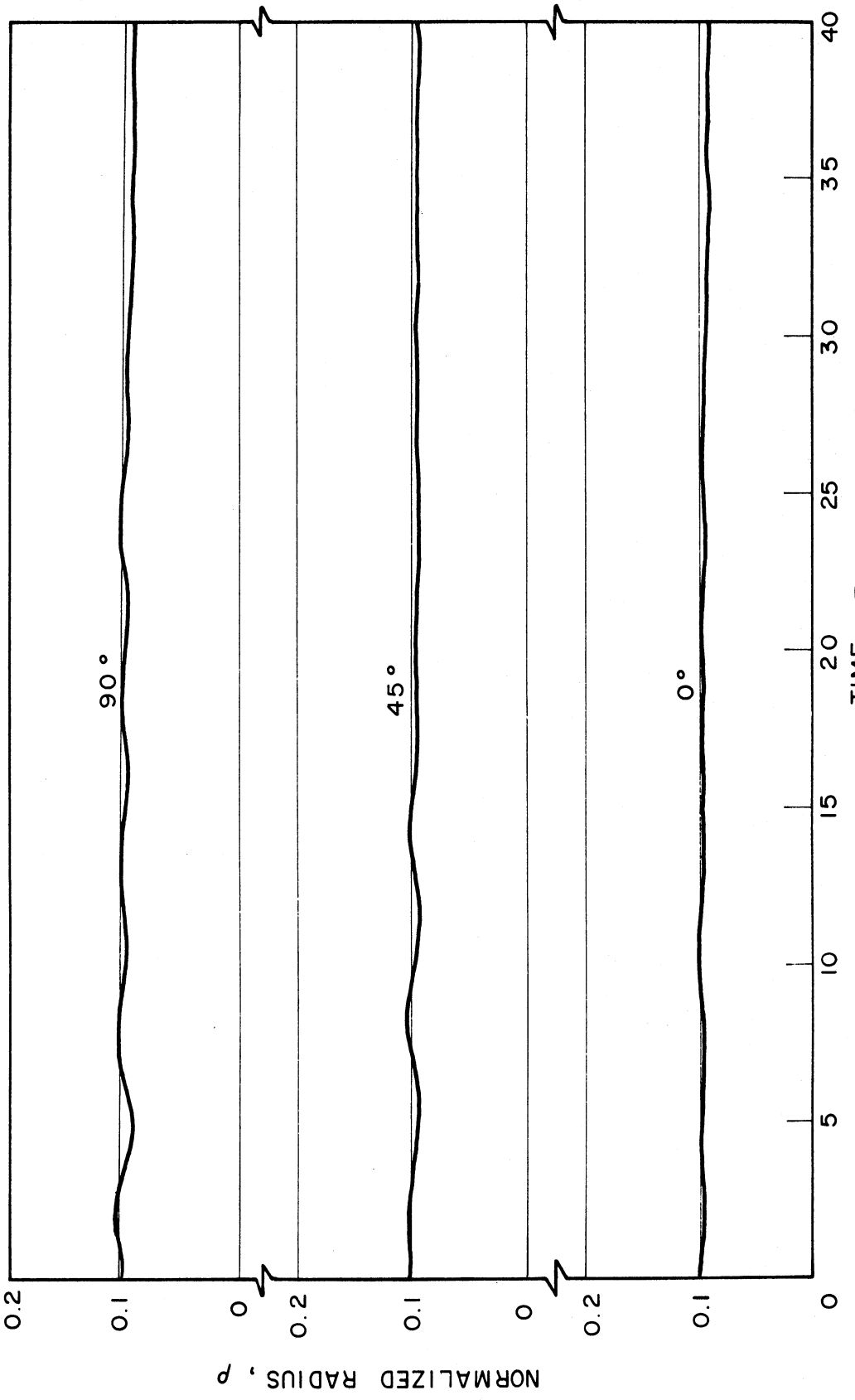

FIG. 3.1 BEAM EXPANSION FOR CYCLOTRON-CYCLOTRON WAVE INTERACTION FOR WEAK PUMP FIELD STRENGTH.

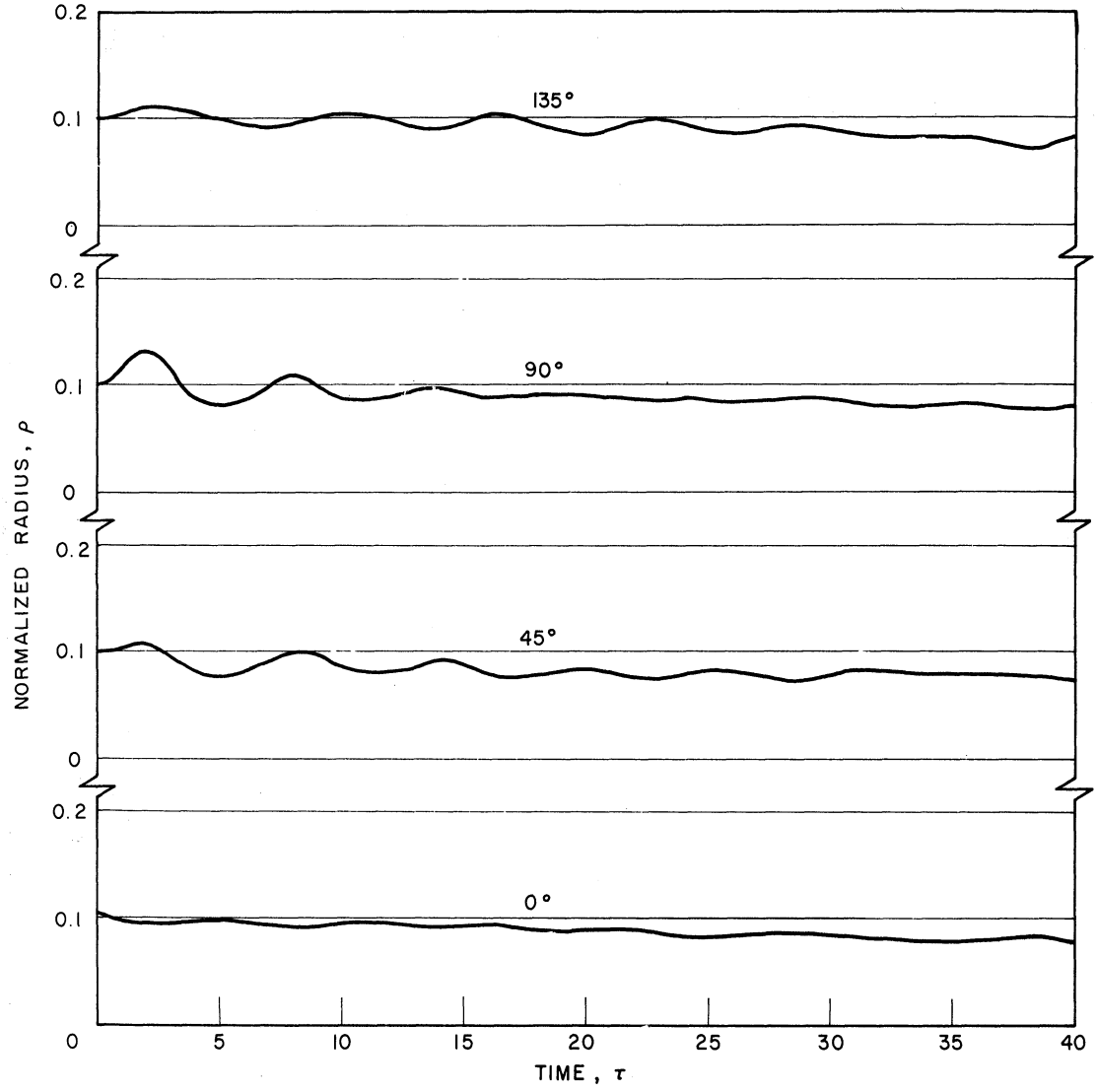

FIG. 3.2 BEAM EXPANSION FOR CYCLOTRON-CYCLOTRON WAVE INTERACTION FOR MEDIUM PUMP FIELD STRENGTH.

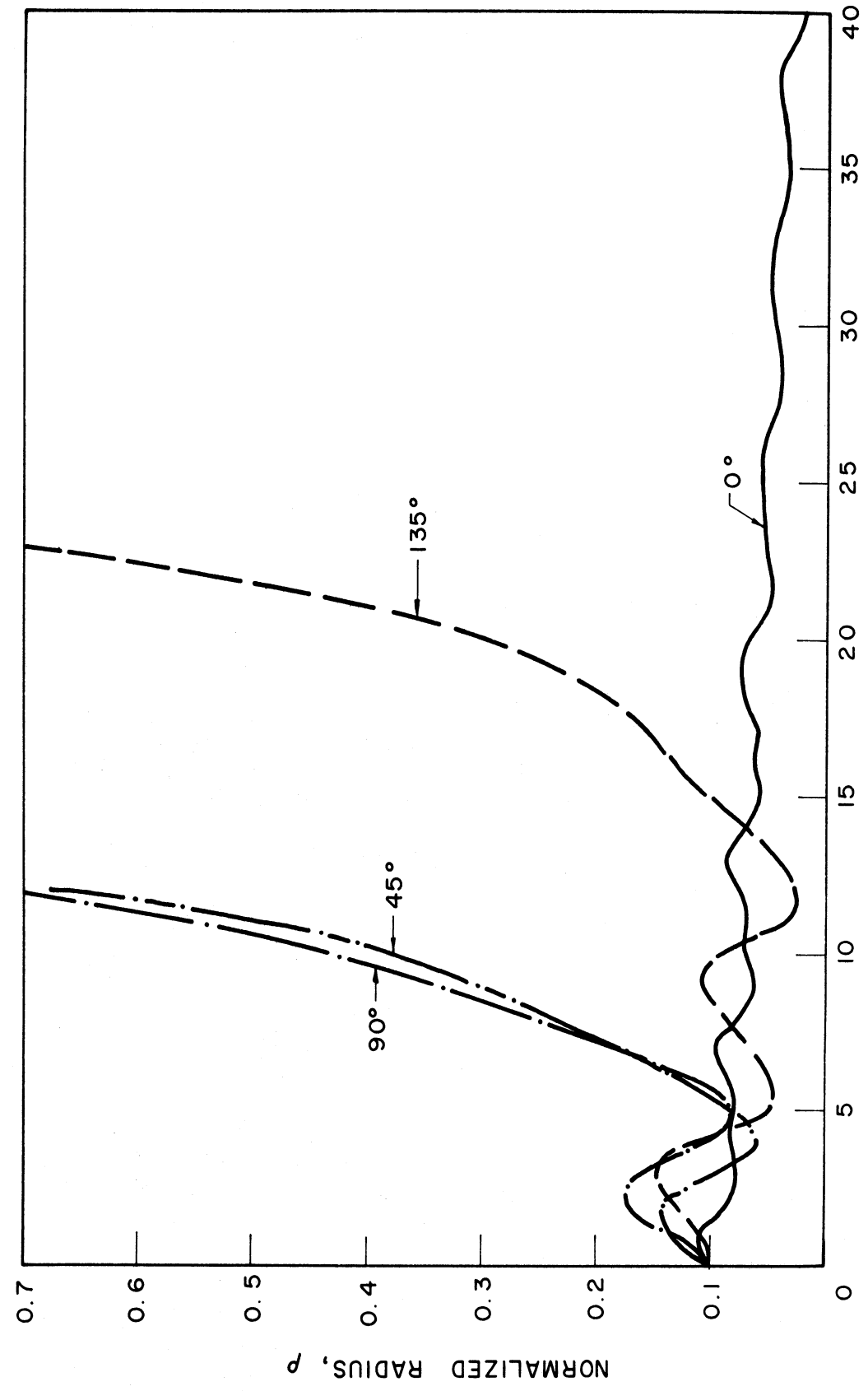

FIG. 3.3 BEAM EXPANSION FOR CYCLOTRON-CYCLOTRON WAVE INTERACTION FOR STRONG PUMP FIELD STRENGTH.

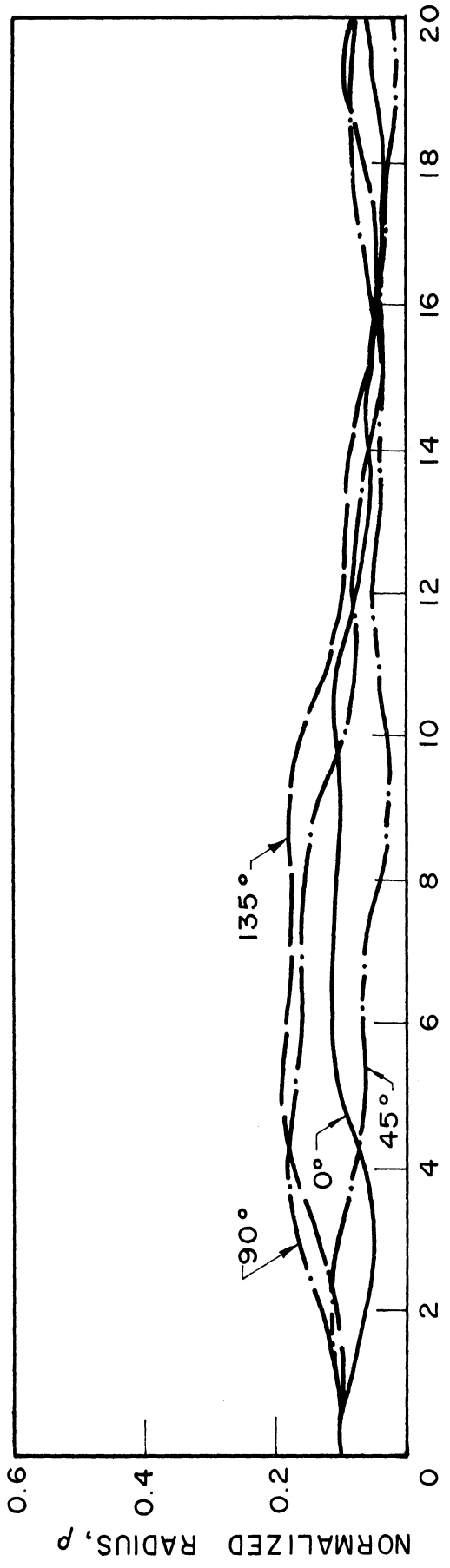

FIG. 3.4 BEAM EXPANSION FOR CYCLOTRON-SYNCHRONOUS WAVE INTERACTION FOR BELOW CRITICAL PUMP FIELD STRENGTH.

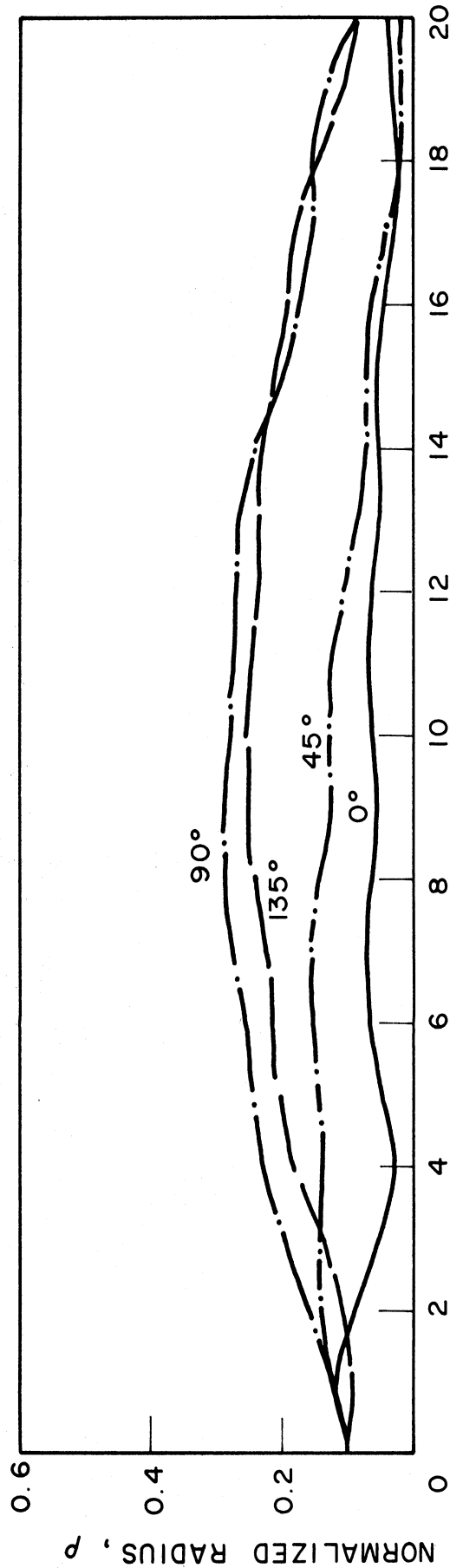

FIG. 3.5 BEAM EXPANSION FOR CYCLOTRON-SYNCHRONOUS WAVE INTERACTION FOR CRITICAL PUMP FIELD STRENGTH.

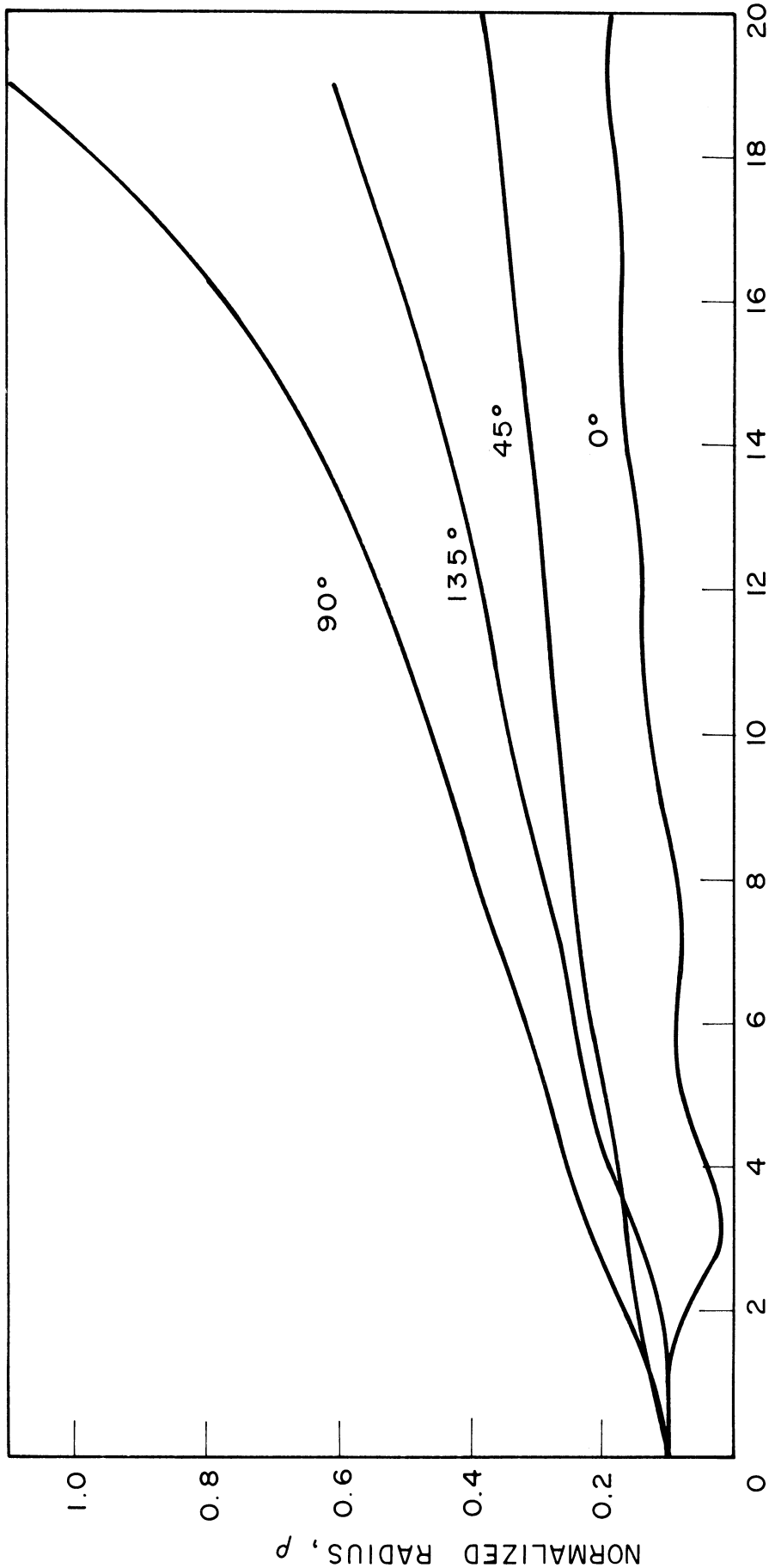

FIG. 3.6 BEAM EXPANSION FOR CYCLOTRON-SYNCHRONOUS WAVE INTERACTION FOR MEDIUM PUMP FIELD STRENGTH.

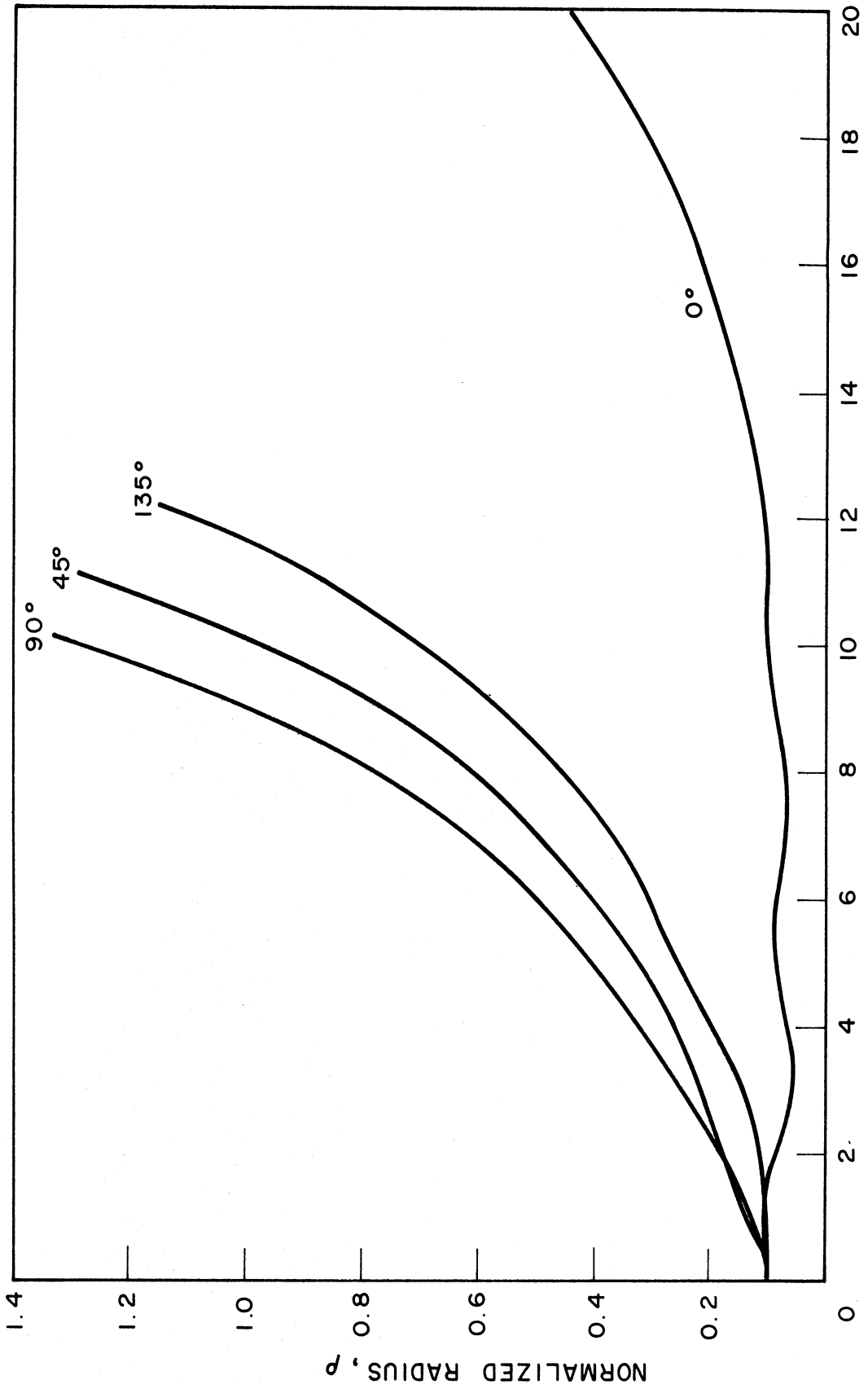

FIG. 3.7 BEAM EXPANSION FOR CYCLOTRON-SYNCHRONOUS WAVE INTERACTION FOR STRONG PUMP FIELD STRENGTH.

(i.e., with an entrance angle of zero or 180 degrees) as soon as it enters the pump field structure.

3.3 The Phase-Focusing Effect. Although a solid unmodulated beam has been assumed when discussing the effects of beam expansion, the actual configuration of the beam entering the pump structure of a transverse-wave amplifier is far from this state. In fact, the beam is initially modulated and $|d\Phi/d\tau|_0 = 0$. The angular location of the previous beam becomes the entrance angle of the beam under consideration. With this modification, trajectories of the beam show a strong phase-focusing effect as is indicated in Figs. 3.8 and 3.9 for the case of cyclotron-cyclotron and cyclotron-synchronous wave interactions, respectively. It is observed that all of the electrons that enter the pump field at different entrance angles in a very short time will align themselves to correspond with the most favorable entrance angle, i.e., the zero-degree entrance angle. Therefore, it is sufficient to say that as far as beam expansion due to the pump field is concerned, only those electrons with a zero-degree entrance angle must be considered. It can be seen from Figs. 3.1 through 3.7 that the beam expansions for all cases with reasonable pump field strengths do not exceed twice the initial value. This indicates that in actual operation the beam expansion due to the pump field should not present a serious problem.

3.4 Program for the Next Quarter. While the experimental tube is being assembled a few more computer studies on the energy relationships and the kinetic power relationships will be investigated.

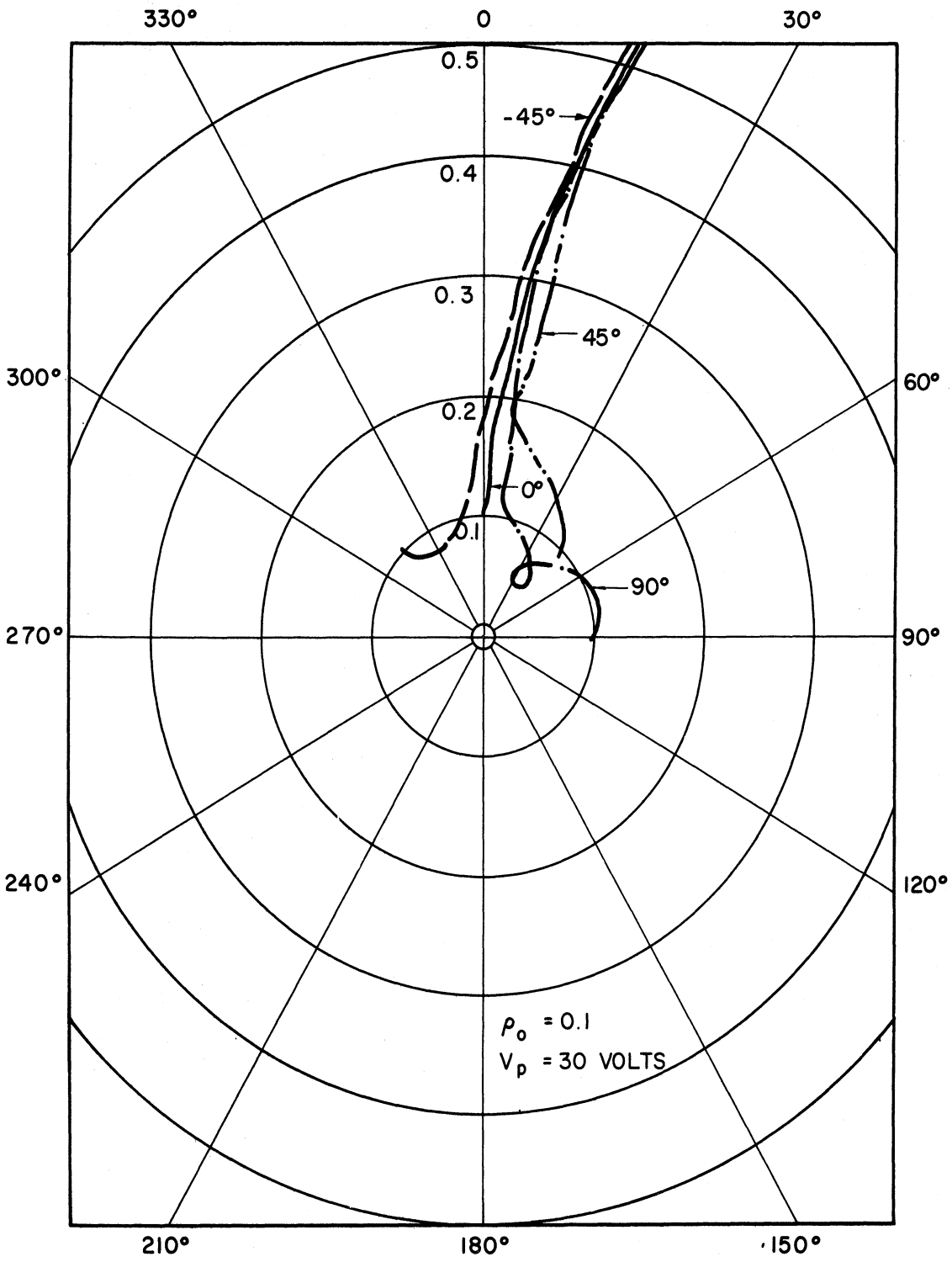

FIG. 3.8 PHASE FOCUSING FOR CYCLOTRON-CYCLOTRON WAVE INTERACTION.

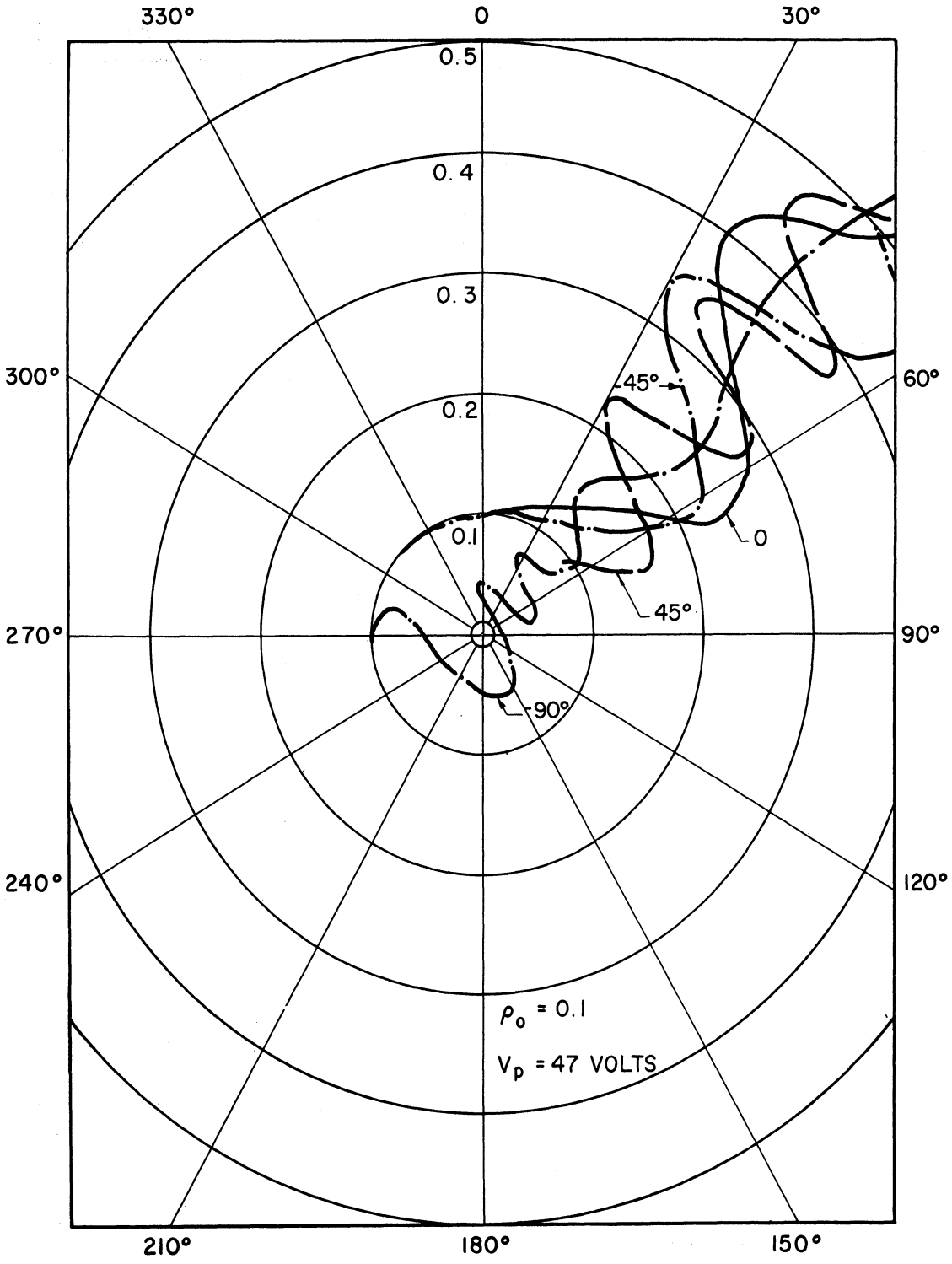

FIG. 3.9 PHASE FOCUSING FOR CYCLOTRON-SYNCHRONOUS WAVE INTERACTION.

4. Investigation of the Cross-Modulation Products in a Wideband Tunnel-Diode Amplifier (C. Yeh)

4.1 Introduction. Equations for predicting the V-I characteristic and the cross-modulation products of a tunnel-diode amplifier have been derived in previous reports (Quarterly Progress Report Nos. 8 and 9). During the present quarter, effort has been devoted to the use of these formulas in the computation of cross-modulation products if a tunnel-diode V-I characteristic curve is given and if two signals are present at the input.

4.2 An Approximation. It has been found that the series expansion used for the hyperbolic tangent function converges very slowly and many terms are needed to accurately simulate the V-I characteristic. This contradicts the statement that one must only consider up to cubic terms of V in the calculations. Fortunately, the range of the V-I characteristic curve for a tunnel diode in amplifier applications is so narrow that the approximation can be justified. It is suggested that for the active range of amplifier application, the hyperbolic tangent function be represented by a straight line, i.e., $\tanh(eV/2kT) \cong m(V_1-V_M)+C$, where the slope $m = \Delta\tanh(eV/2kT)/(V_1-V_M)$, $C = \tanh(eV_M/2kT)$, and V_1 is the value of V such that $\tanh(eV_1/2kT) \simeq 1$. To prove that such an approximation is actually tolerable, the negative resistance range of the V-I characteristic of a tunnel diode is calculated and plotted as circles along with the exact characteristic curve of the diode and is shown in Fig. 4.1. It is seen that the agreement is fairly good.

4.3 The Cross-Modulation Products. By means of the above approximation, the equation for the diode current can be rewritten as

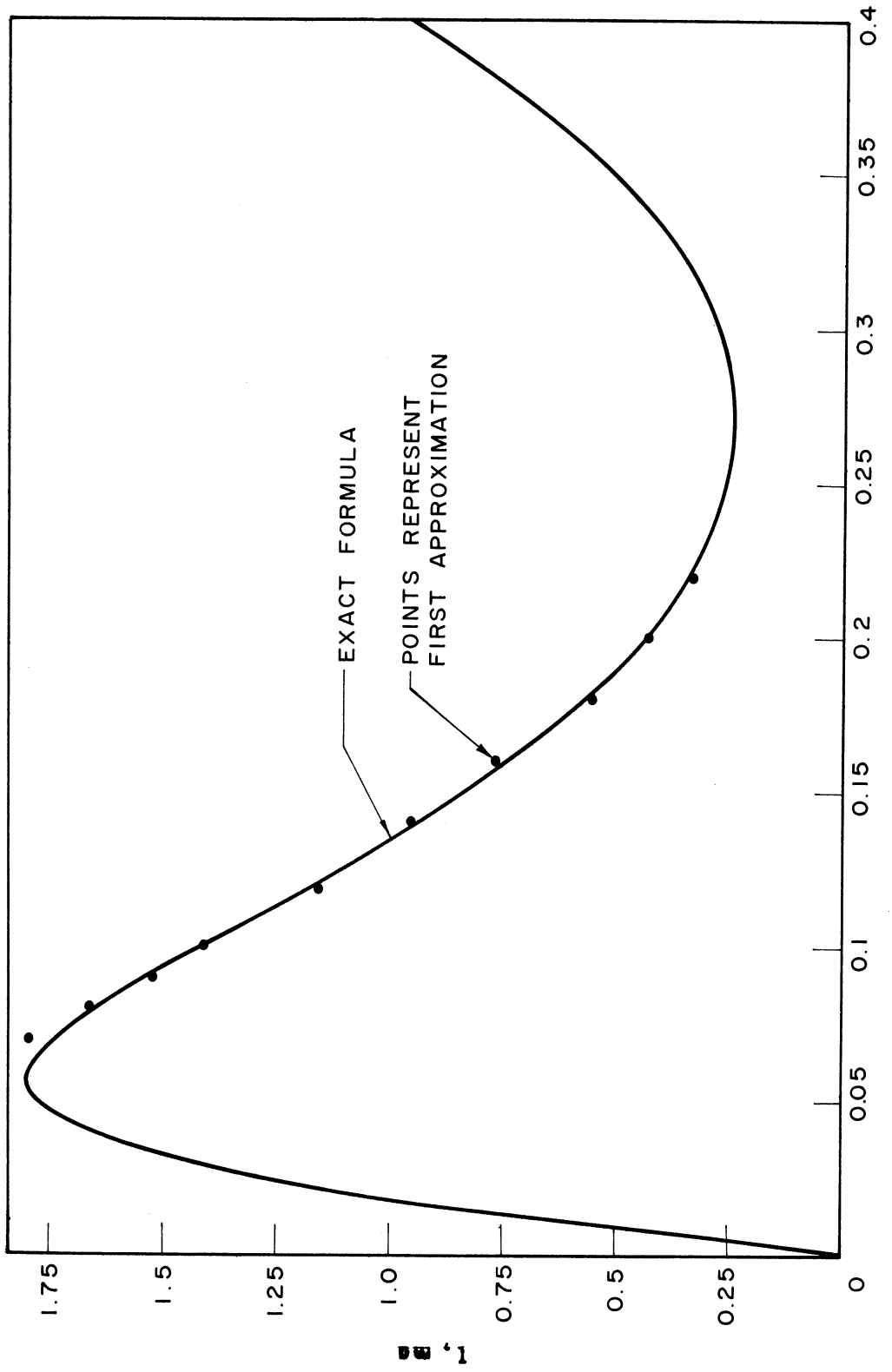

FIG. 4.1 COMPUTED STATIC CHARACTERISTIC OF A TUNNEL DIODE.

$$J = a(V_m - V)^2 [m(V - V_M) + C] + g_o V$$

$$= C_o + C_1 V + C_2 V^2 + C_3 V^3 \quad , \tag{4.1}$$

where

$$C_o = aV_m^2(C - mV_M) \quad ,$$

$$C_1 = [amV_m^2 + g_o - 2aV_m(C - mV_M)] \quad ,$$

$$C_2 = a[(C - mV_M) - 2mV_m] \quad ,$$

$$C_3 = am$$

and

$$a = (J_M - g_o V_M)/(V_m - V_M)^2 \tanh eV_M/2kT \quad . \tag{4.2}$$

Let

$$V = a_o + a_1 \cos \omega_1 t + a_2 \cos \omega_2 t \quad , \tag{4.3}$$

where a_o is actually the d-c bias voltage and a_1 and a_2 are the amplitudes of the two input signals.

By means of Tables 4.1 through 4.4 in Quarterly Progress Report No. 9, the modulation product contributions due to the quadratic and cubic terms can be written out and when they are multiplied by the appropriate constants and summed according to Eq. 4.1, with omission of the frequencies out of the bandwidth of the wideband amplifier, the following components result. The current component of fundamental frequency, ω_1, is

$$J_{\omega_1} = a_1\left[C_1 + 2a_o C_2 + 3C_3\left(a_o^2 + \frac{1}{4} a_1^2 + \frac{1}{2} a_2^2\right)\right] \tag{4.4}$$

and the current component at the fundamental frequency, ω_2, is

$$J_{\omega_2} = a_2\left[C_1 + 2a_0C_2 + 3C_3\left(a_0^2 + \frac{1}{4}a_2^2 + \frac{1}{2}a_1^2\right)\right] \tag{4.5}$$

The current components of $2\omega_1-\omega_2$ and $2\omega_2-\omega_1$ are, respectively,

$$J_{2\omega_1-\omega_2} = \frac{3}{4}a_1^2a_2C_3 \tag{4.6}$$

and

$$J_{2\omega_2-\omega_1} = \frac{3}{4}a_1a_2^2C_3 \tag{4.7}$$

The d-c component, the difference frequency $\omega_1-\omega_2$, the second harmonic frequency components $2\omega_1$ and $2\omega_2$, and the sum frequency components $\omega_1+\omega_2$, $2\omega_1+\omega_2$ and $\omega_1+2\omega_2$ are assumed to be out of the bandwidth of the amplifier.

Figures 4.2 and 4.3 are the results of calculations for two operating conditions of a tunnel-diode amplifier. In each figure, the ratio of the signal amplitudes, a_2/a_1, is used as a variable. The signal outputs at different frequencies are plotted as a function of a_2/a_1. In Fig. 4.2, the bias voltage is 0.13 and the maximum amplitude of a_1 is 0.04. In Fig. 4.3, the bias voltage is 0.14 and the maximum amplitude of a_1 is 0.07.

The results of the calculations can be summarized as follows:

a. The amplitude of one of the signals, ω_1, decreases slightly as the amplitude of the other signal, ω_2, increases.

b. The amplitude of the difference frequency, $2\omega_2-\omega_1$, is the largest among the modulation products within the bandwidth. It increases with

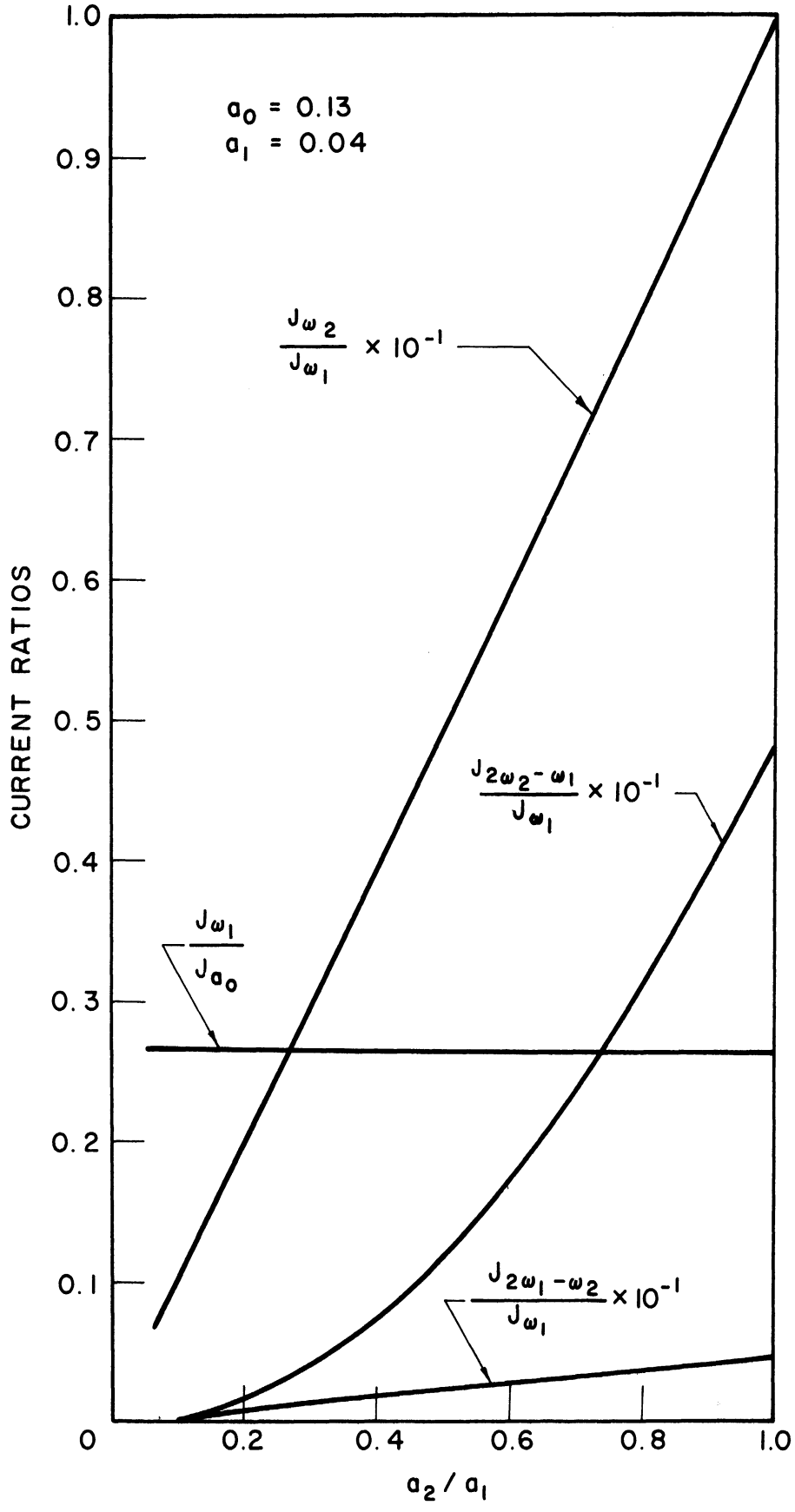

FIG. 4.2 CROSS-MODULATION OUTPUT AT DIFFERENT FREQUENCIES AS A FUNCTION OF a_2/a_1 FOR $a_0 = 0.13$ AND $a_1 = 0.04$.

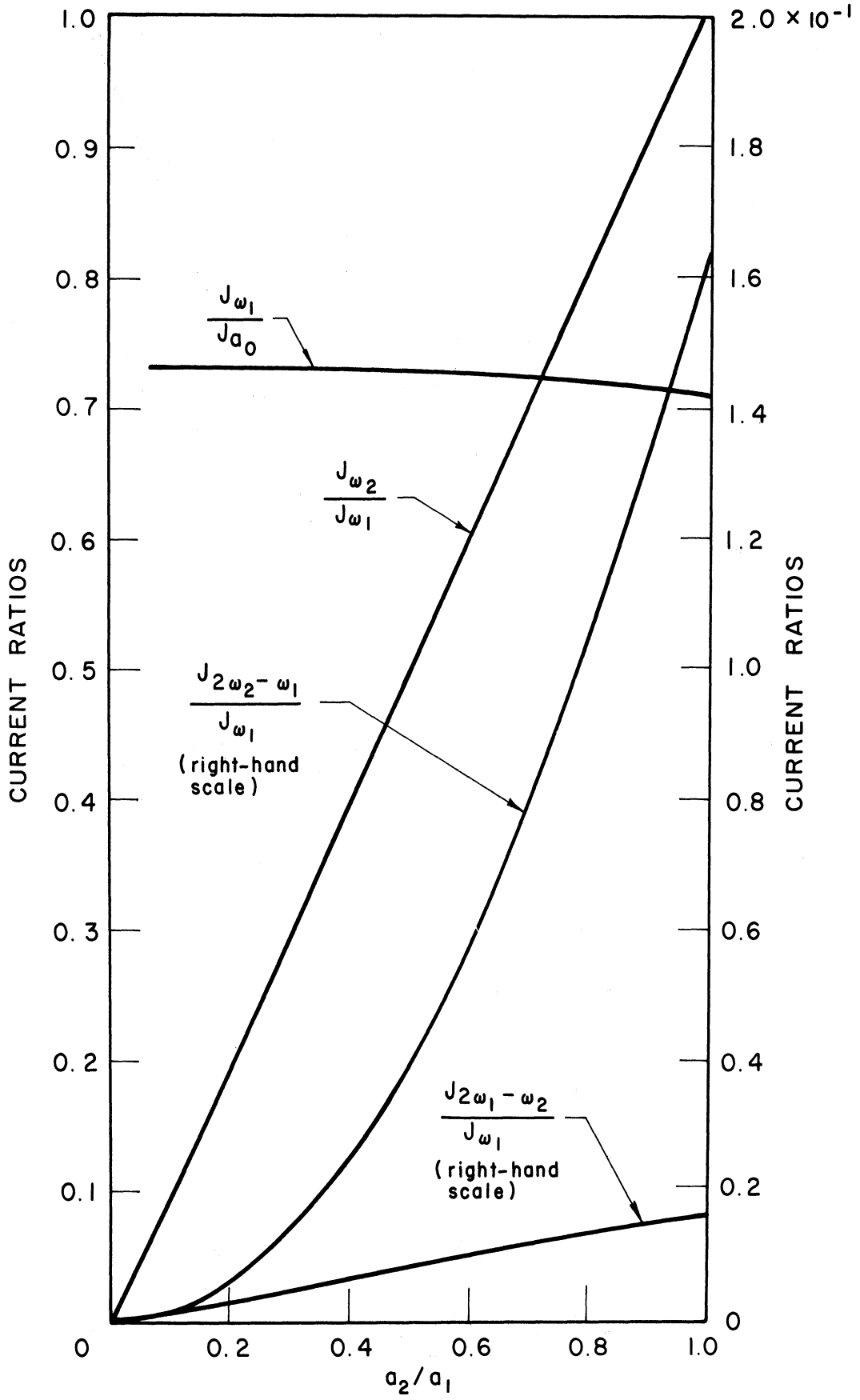

FIG. 4.3 CROSS-MODULATION OUTPUT AT DIFFERENT FREQUENCIES FOR $a_o = 0.14$ AND $a_1 = 0.07$.

a_2/a_1 almost quadratically and is larger than the amplitude of the $2\omega_1-\omega_2$ component.

c. The ratio $J_{2\omega_2-\omega_1}/J_{2\omega_1-\omega_2}$ varies almost linearly with a_2/a_1. The effect of changing the operating point does not seem to change this ratio appreciably.

d. The bias and the signal amplitudes are small so that no gross nonlinear effects are observed.

4.4 Program for the Next Quarter. Computation of the modulation products will be continued to include the case of a large bias and strong signal amplitudes. The products due to three-signal inputs will also be studied. A wideband X-band tunnel-diode amplifier has been ordered and experimental measurements of the modulation products will be made and the results compared with those obtained theoretically.

5. Experimental Characteristics of Multisignal Traveling-Wave Amplifiers

(N. A. Masnari)

5.1 Experimental Investigation. The experimental multisignal investigations are concerned with the interaction phenomenon occurring in a microwave tube when several r-f signals are applied simultaneously to the tube. Because of the nonlinear nature of the interaction process in a microwave tube, various cross-modulation terms are generated. The relationship of these difference-frequency signals to various parameters is of special interest. Whenever possible it is also important to study the harmonic-frequency terms which result from the beam-wave interaction process.

Although the multisignal operation of traveling-wave amplifiers is of interest over the entire microwave frequency range, the results described herein are concerned only with the 100-300 mc range. The

device under study is a UHF Crestatron developed through the combined efforts of the Electron Physics Laboratory and the Bendix Corporation[1]. The tube is capable of generating in excess of 100 watts of cw power with a beam current of 450-500 ma. The beam is formed by a hollow cathode and is confined by magnetic focusing. A helix is used for the slow-wave circuit. The large operating powers require the use of a water-cooled collector. Figure 5.1 is a schematic diagram of the tube which, in general, has an operating beam voltage of 1150 volts.

5.2 Single-Frequency Operation. The purpose of the initial investigation was to evaluate the Crestatron operation with only a single frequency applied at the input. The investigation was concerned both with the fundamental frequency output and with the second harmonic (and the third harmonic when observable). The frequency and the power level of the input signal were varied and the output was evaluated over the operating range. Figure 5.2 illustrates the test setup for the experimental evaluation of the operation.

The fundamental, second-harmonic and third-harmonic power outputs are plotted in Fig. 5.3a as a function of the input power, P_i, for f_1 = 100 mc, V_k = 1050 volts and I_k = 450 ma. Figure 5.3b illustrates the gain in db as a function of P_i. The fundamental has a maximum gain of approximately 12 db at P_i = 5 dbw, while the second harmonic has its maximum value of 7.5 db at approximately the same input power. The maximum third-harmonic gain is approximately 1 db and occurs at higher power levels. In general the second harmonic for this case is 4-5 db

---

1. Earl, K. C. et al., "Development of 100-Watt Crestatron Amplifier for Operation in the 100-300 Megacycle Frequency Range", Final Tech. Report Part II, Report No. 2893, The Bendix Corporation, Research Laboratories Division, Southfield, Mich.

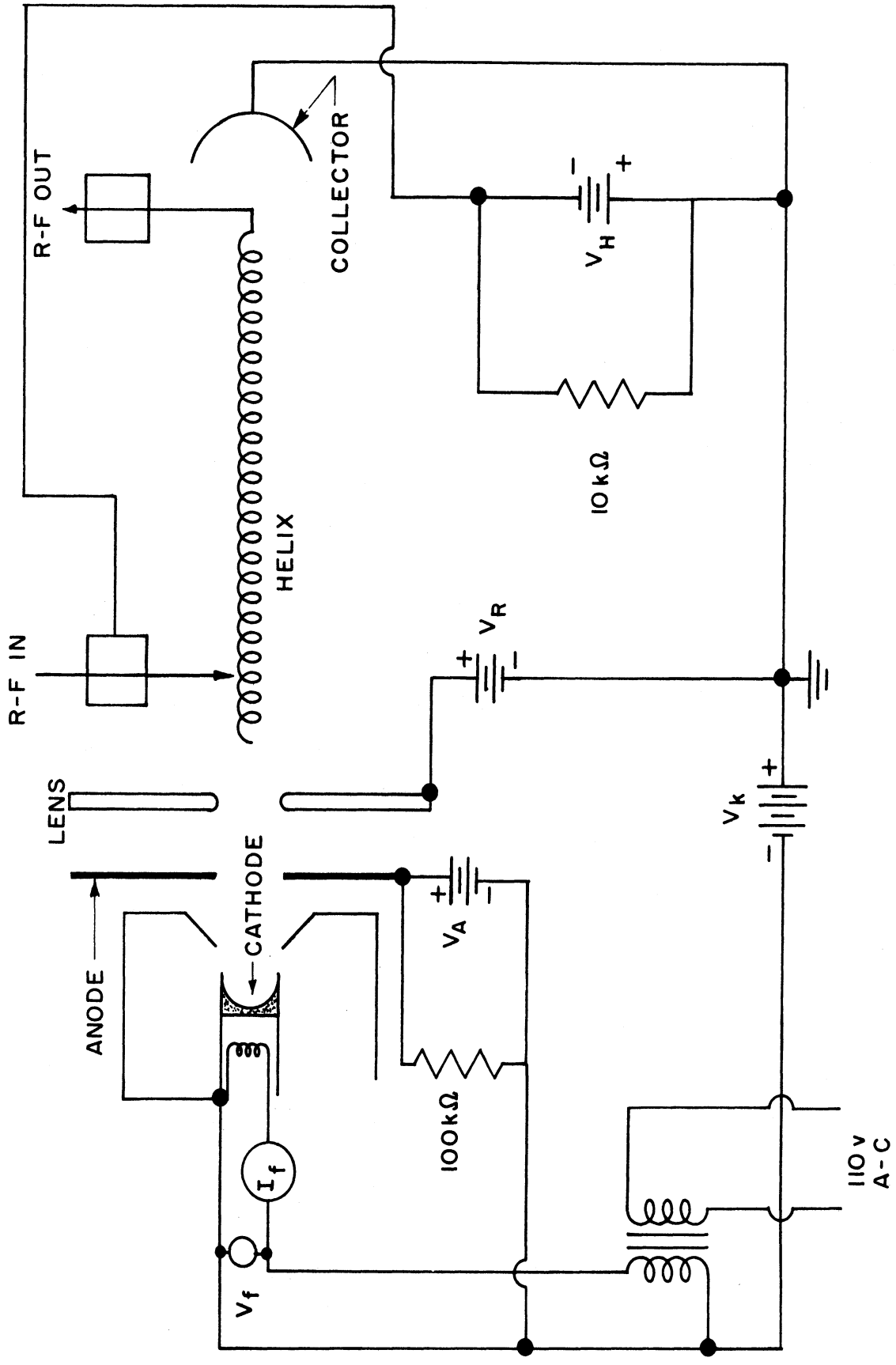

FIG. 5.1 SCHEMATIC DIAGRAM OF THE UHF CRESTATRON.

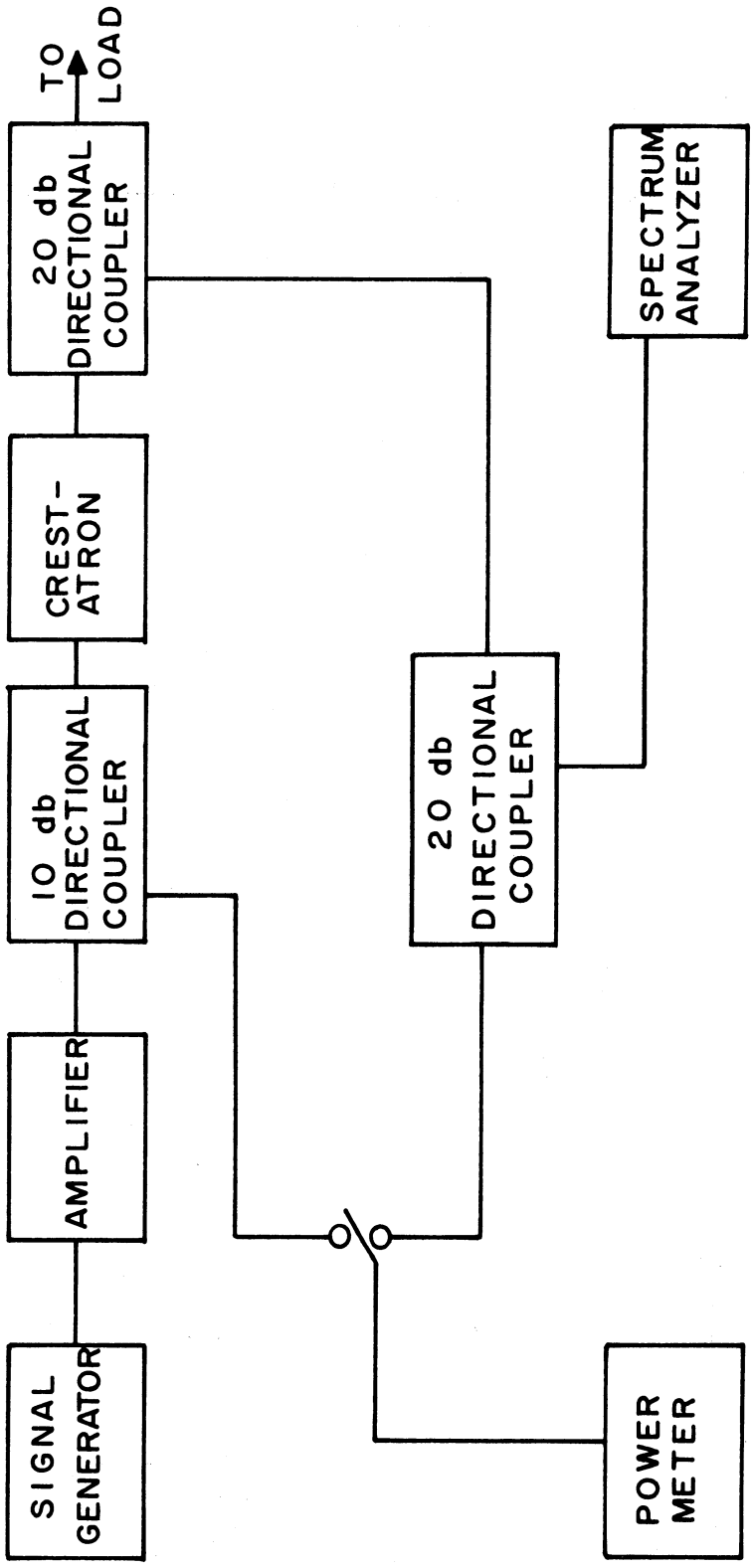

FIG. 5.2 TEST SETUP FOR SINGLE-FREQUENCY INVESTIGATIONS.

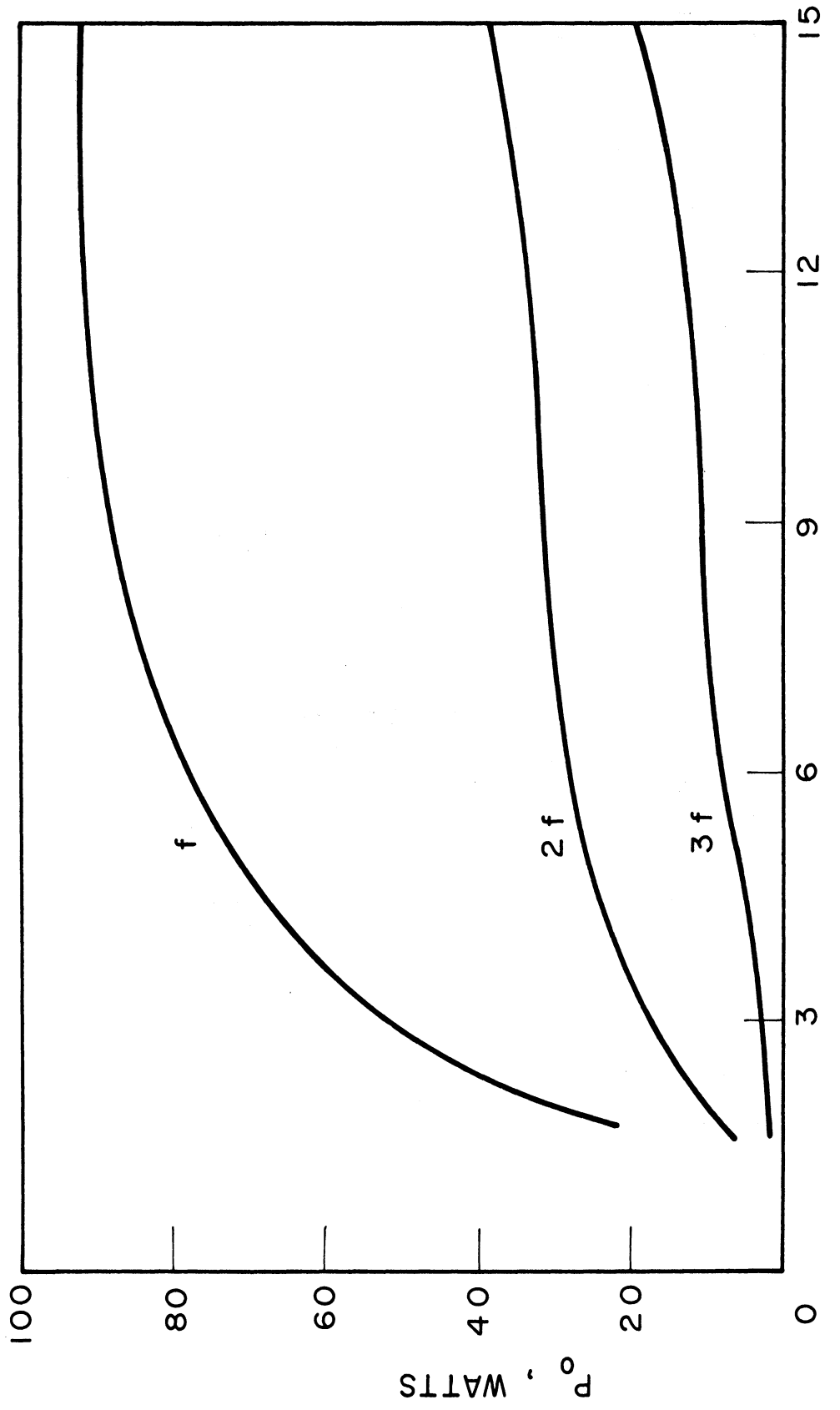

FIG. 5.3a FUNDAMENTAL AND HARMONIC POWER OUTPUTS AS A FUNCTION OF THE INPUT POWER. (f = 100 mc, I_k = 450 ma, V_k = 1050 VOLTS)

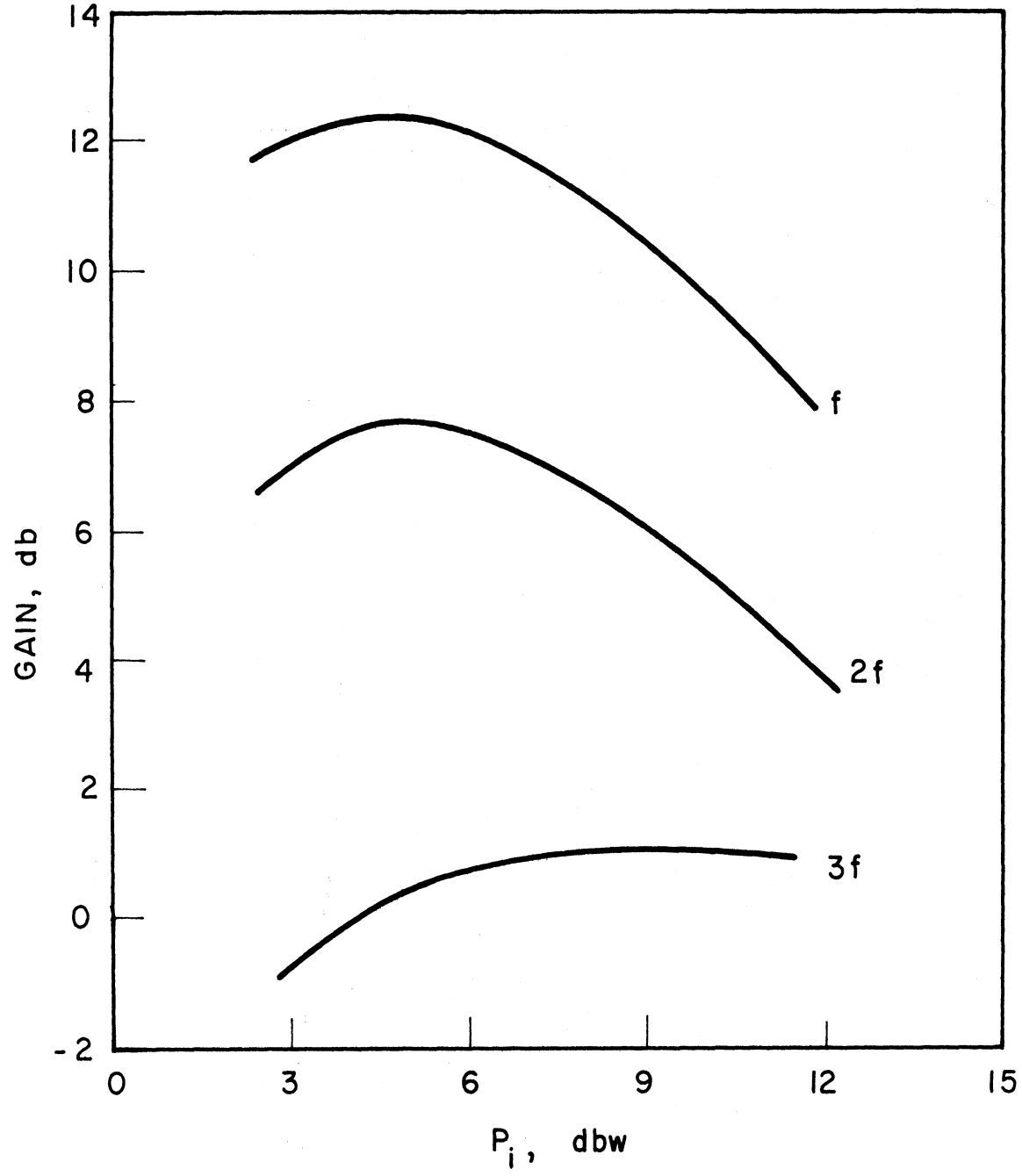

FIG. 5.3b FUNDAMENTAL AND HARMONIC GAIN CURVES. (f = 100 mc, I_k = 450 ma, V_k = 1040 VOLTS)

below the fundamental over the entire P_i range. The third harmonic is down 3-6 db with respect to the second harmonic.

Similar results are illustrated in Figs. 5.4 and 5.5 for f = 120 mc and f = 140 mc respectively. The general results are the same, with the second harmonic being down anywhere from 5-12 db with respect to the fundamental. In each case it is observed that the fundamental experiences a maximum gain at some particular P_i value and then decreases. It was also observed, although not illustrated here, that there were significant oscillations for an input signal of 110 mc.

Figure 5.6 indicates the maximum gain for the fundamental and the second harmonic as a function of the applied r-f signal frequency. It is apparent that the fundamental has its maximum gain (in the range between 100 and 150 mc) of 15 db at f = 120 mc. The second harmonic has its maximum gain (8 db) at approximately 130 mc when the gain of the fundamental is only 12 db.

5.3 Multisignal Operation. The single-frequency investigation was followed by a study of the tube performance when two signals were simultaneously applied to the Crestatron. The frequency and the power level of each signal were independently variable, thus allowing investigation of the nonlinear operation over the entire 100-300 mc frequency range. Figure 5.7 illustrates the circuit used for this investigation.

When two signals with frequencies f_1 and f_2 are applied simultaneously to the tube, the output contains various components in addition to those at the applied frequencies; e.g., the cross-modulation terms $2f_1-f_2$, $2f_2-f_1$, etc., are also present. The output cross-modulation signals at frequencies $2f_1-f_2$ and $2f_2-f_1$ are particularly interesting. Second harmonics of f_1 and f_2 are also present but they can be discerned only when $2f_1$ and $2f_2$ are less than 300 mc.

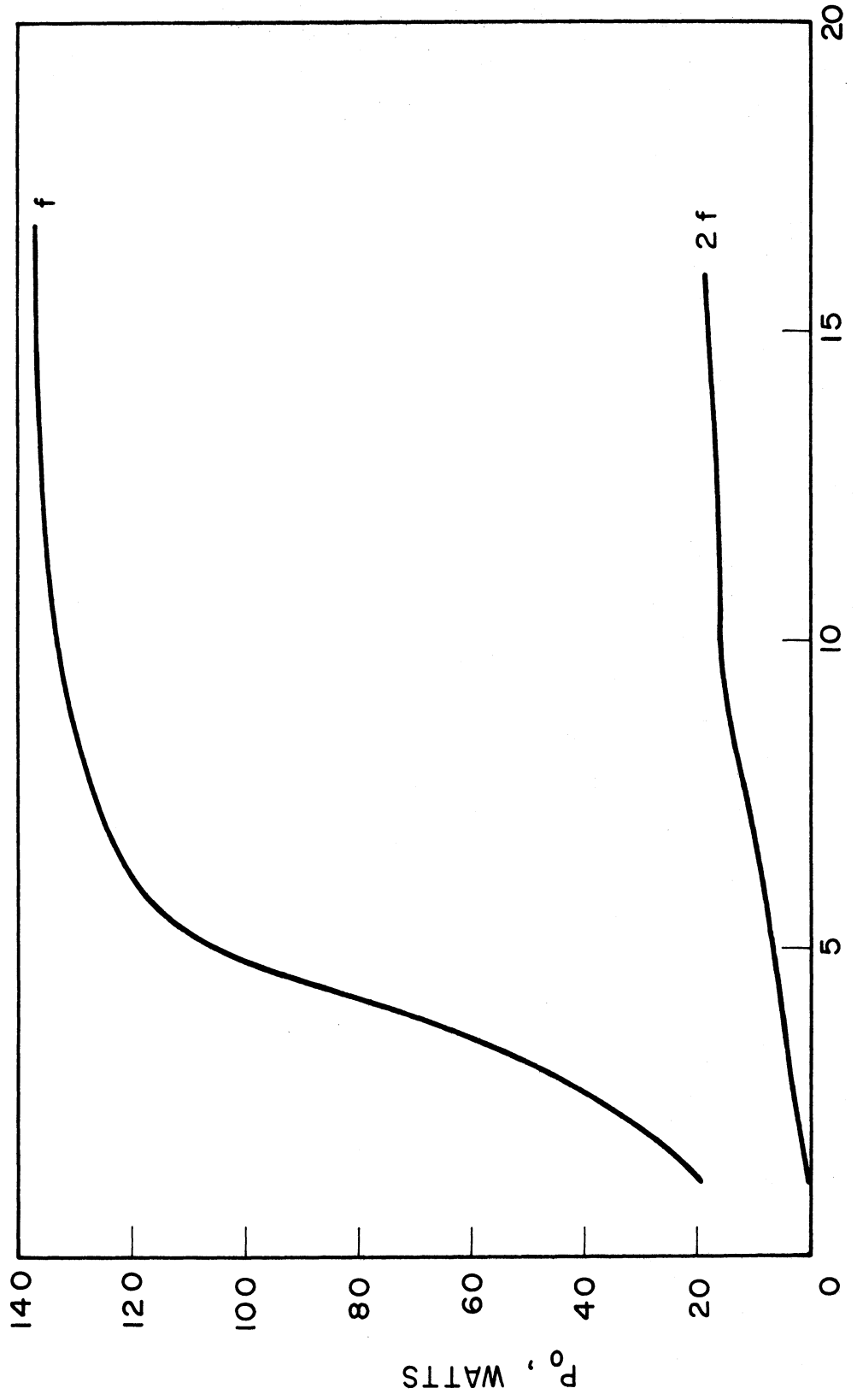

FIG. 5.4 FUNDAMENTAL AND SECOND-HARMONIC POWER OUTPUTS. (f = 120 mc, I_k = 450 ma, V_k = 1050 VOLTS)

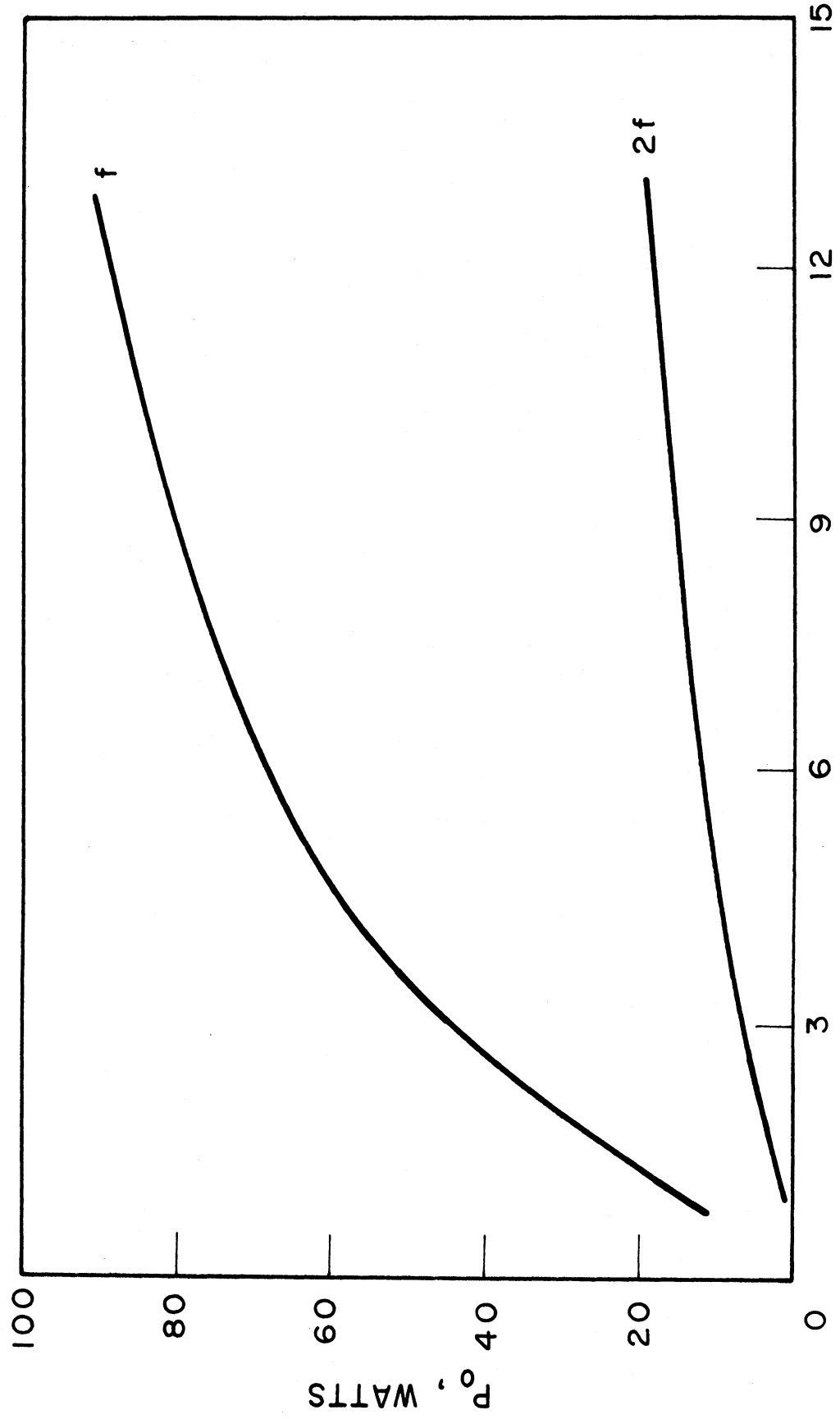

FIG. 5.5 FUNDAMENTAL AND SECOND-HARMONIC POWER OUTPUTS. (f = 140 mc, I_k = 450 ma, V_k = 1050 VOLTS)

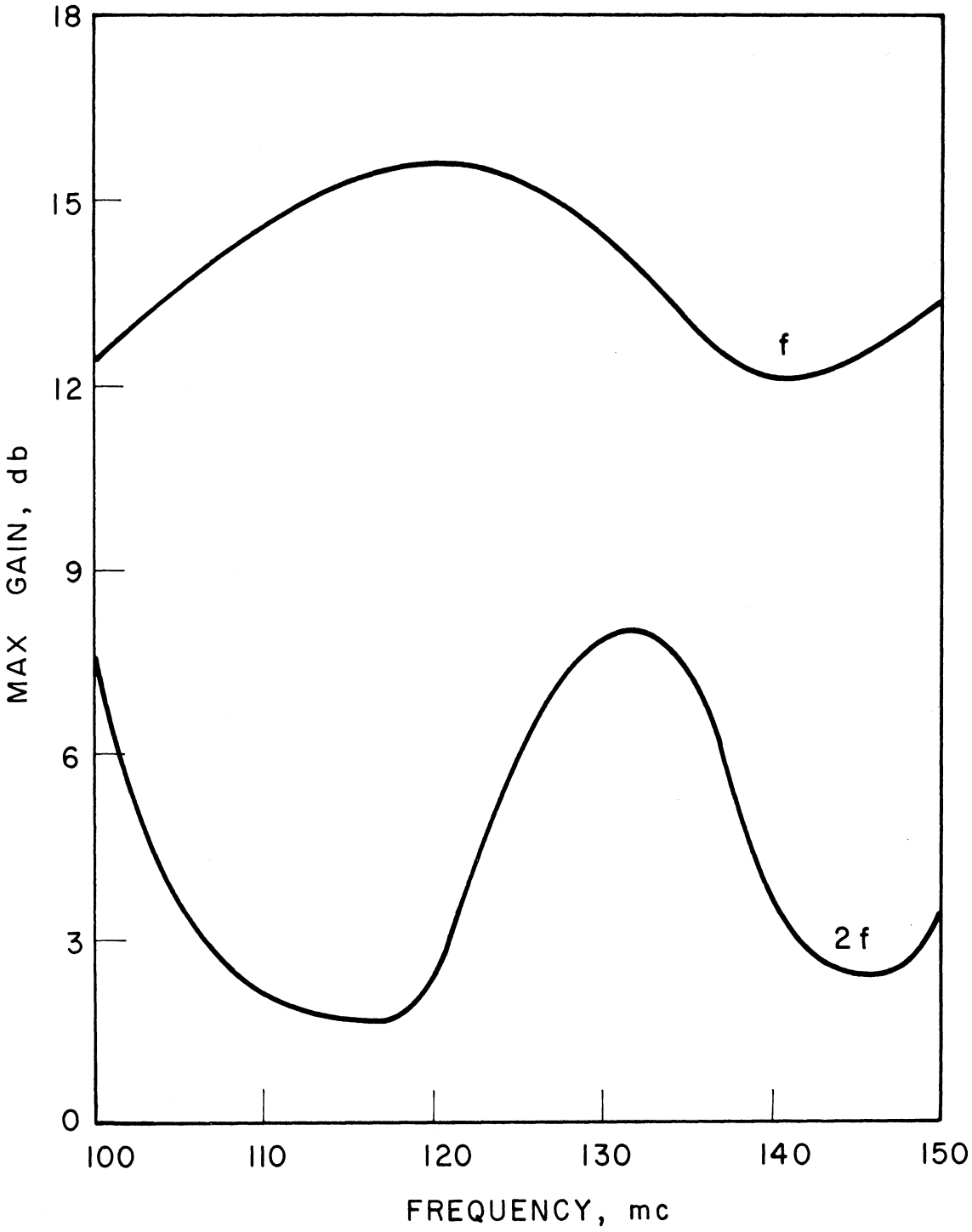

FIG. 5.6 MAXIMUM GAIN AS A FUNCTION OF FREQUENCY FOR THE FUNDAMENTAL AND SECOND-HARMONIC POWER OUTPUTS. (I_k = 450 ma, V_k = 1050 VOLTS)

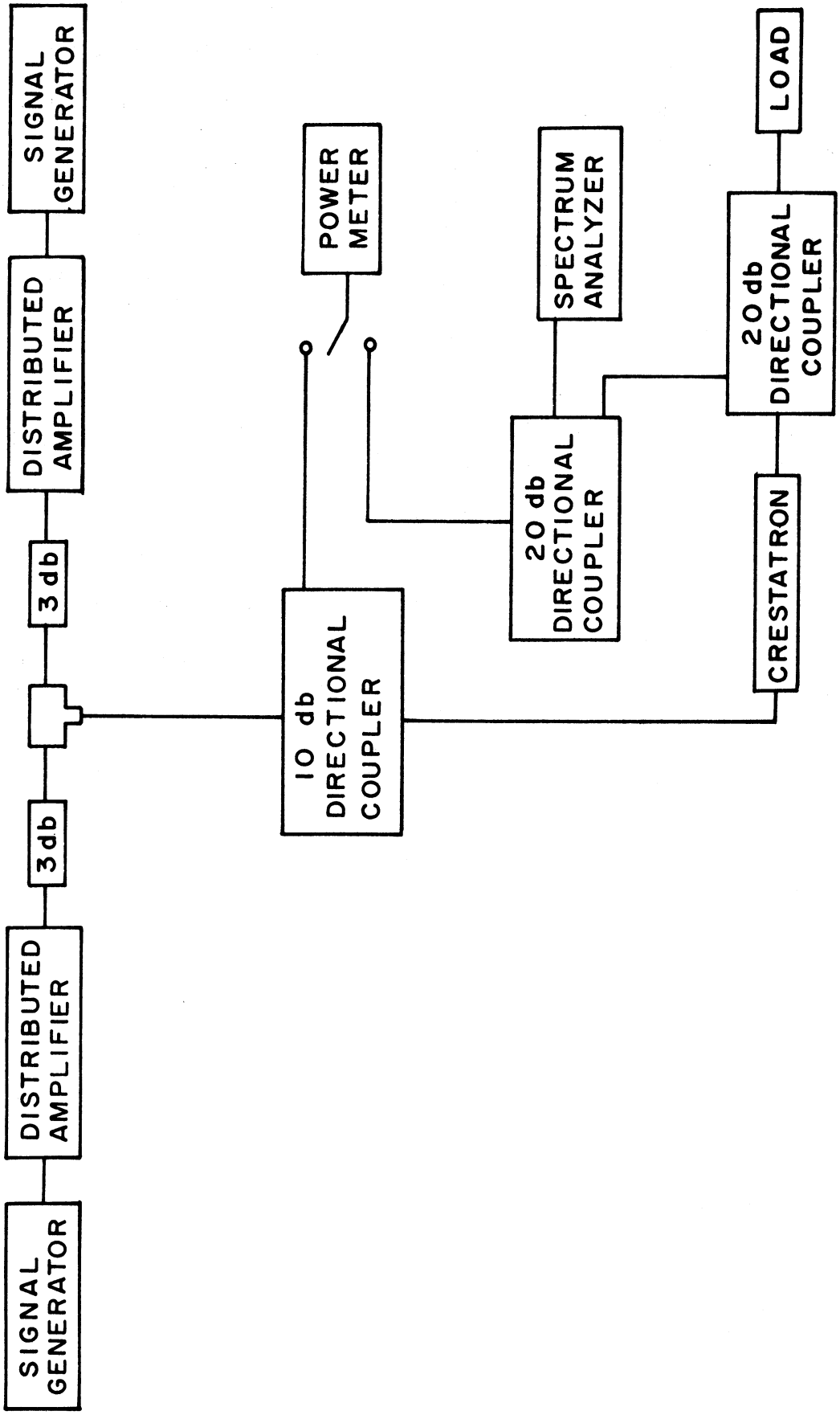

FIG. 5.7 TEST SETUP FOR THE MULTISIGNAL CRESTATRON INVESTIGATIONS.

Figure 5.8 illustrates the situation in which signal 1 is applied at f_1 = 120 mc with an input level of P_{1i} = 15 watts. A second variable amplitude signal is applied at f_2 = 140 mc. As P_{2i} is increased, the output power at $f_2(P_{2O})$ increases as expected. However, the output signal P_{1O} at f_1 and its second harmonic $2f_1$ decrease as P_{2i} increases. This behavior results directly from the nonlinear beam-wave interaction which removes some of the energy from f_1 and $2f_1$. The cross-modulation term at $2f_1-f_2$ is negligible until P_{2i} = 1 watt when it appears with a value of 2 watts. The other term, $2f_2-f_1$, never achieves any measurable value.

Figure 5.9 illustrates a similar result when f_1 and f_2 are increased to 140 mc and 160 mc respectively. P_{1i} is fixed at a level of 10.5 watts while P_{2i} is varied between zero and two watts. Again, P_{1O} and its second-harmonic term decrease as P_{2i} is increased. The signal at $2f_1-f_2$ increases with P_{2i} until it reaches a value of four watts at P_{2i} = 2 watts. The $2f_2-f_1$ term also appears with a power of 1.5 watts for P_{2i} = 2 watts.

With P_{1i} fixed at 10.5 watts, it is observed that as f_1 and f_2 are increased, the cross-modulation term $2f_1-f_2$ becomes larger and eventually is comparable to P_{2O}. This is illustrated in Fig. 5.10 for f_1 = 260 mc, f_2 = 280 mc and P_{1i} = 13 watts. At P_{2i} = 2 watts the power at $2f_1-f_2$ is approximately 6.5 watts as compared to P_{2O} = 6 watts.

From the above data it is apparent that when a large signal is applied to the tube at a given frequency f_1, the application of a second smaller signal at $f_2 > f_1$ results in the generation of the cross-modulation term $2f_1-f_2$ which is at a lower frequency than f_1.

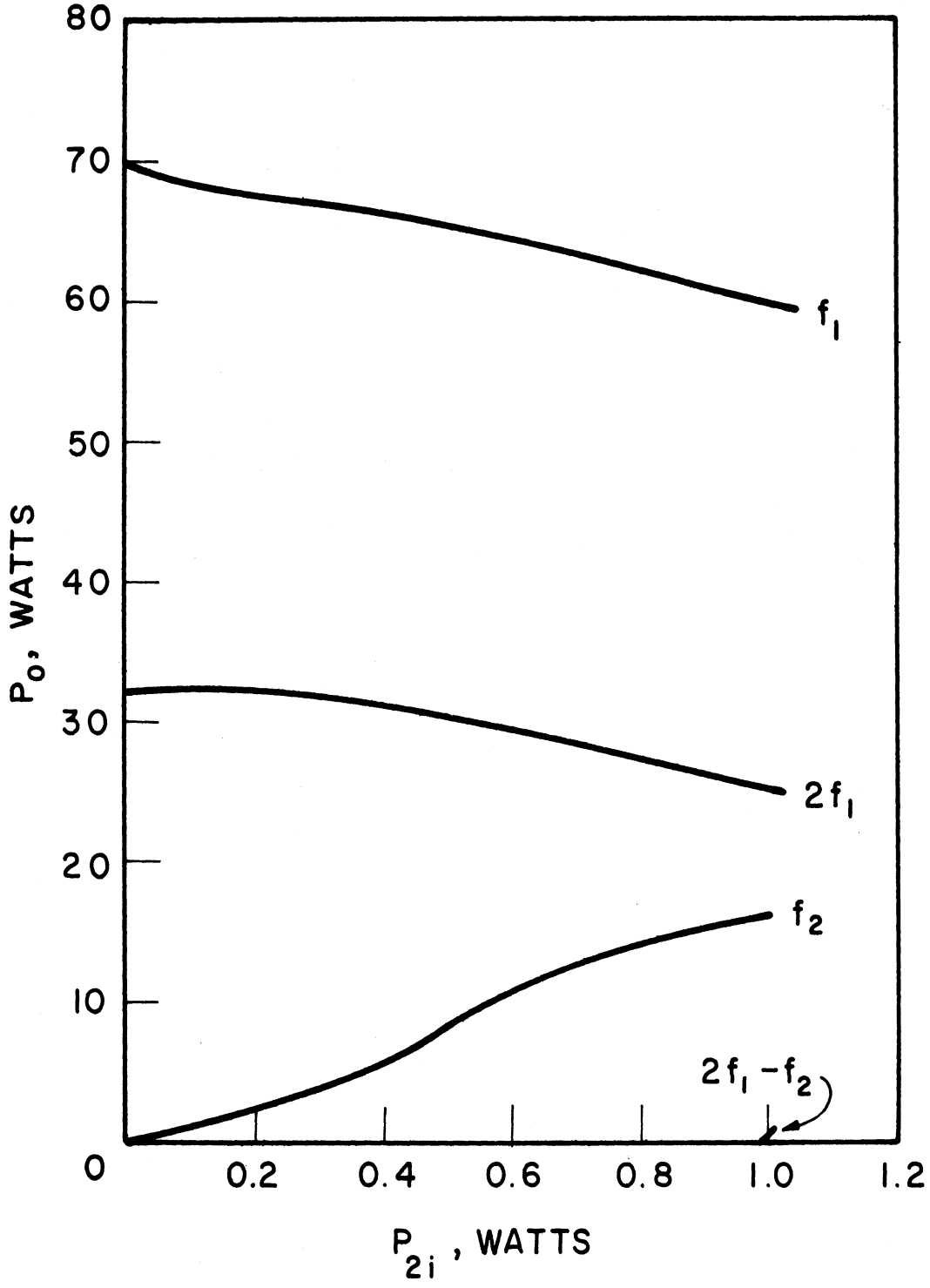

FIG. 5.8 OUTPUT POWERS OF VARIOUS SIGNALS WHEN THE INPUT POWER AT f_2 IS VARIED. (f_1 = 120 mc, f_2 = 140 mc, P_{1i} = 15 WATTS, P_{2i} IS VARIABLE)

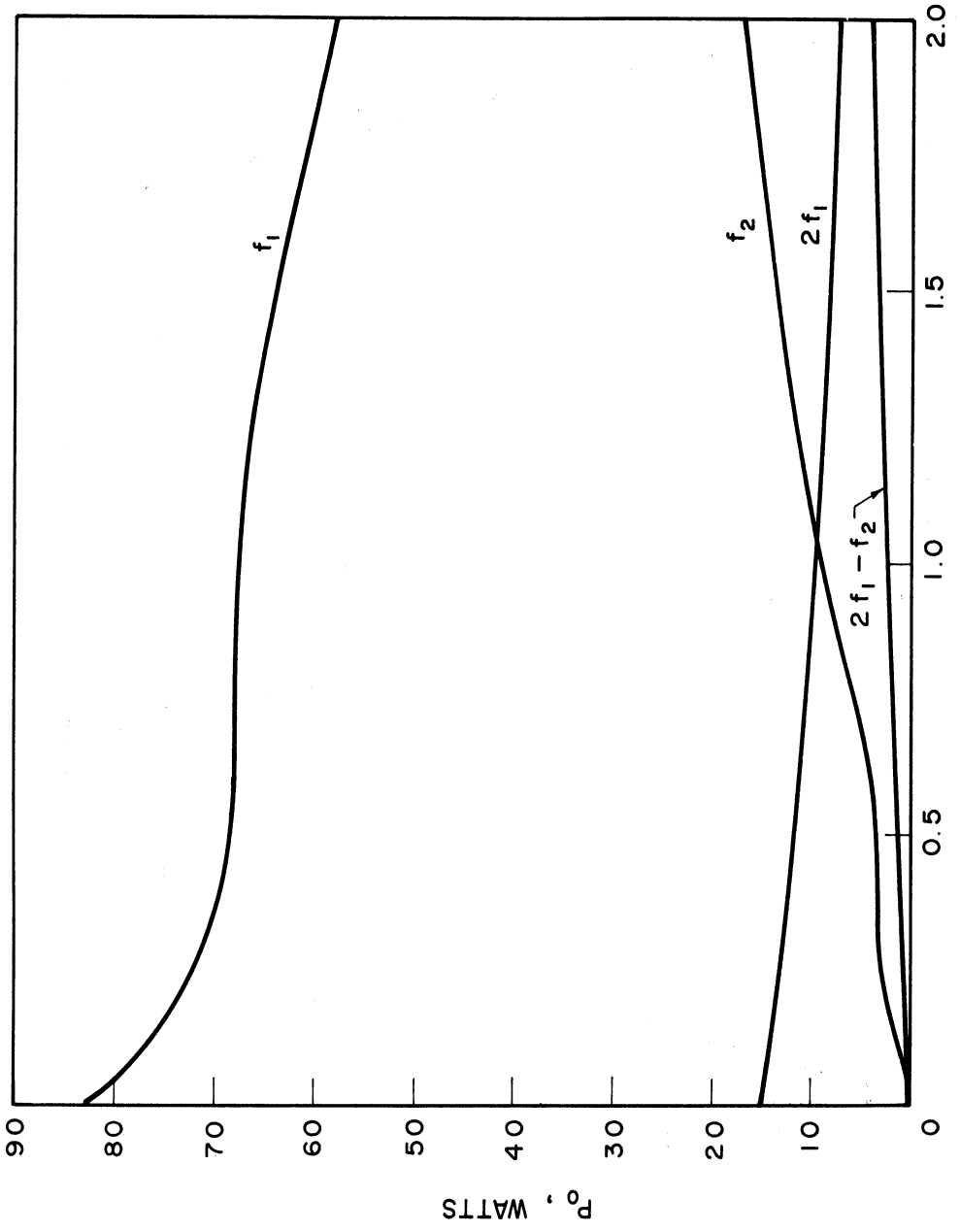

FIG. 5.9 OUTPUT POWERS AS THE f_2 INPUT POWER IS VARIED. (f_1 = 140 mc, f_2 = 160 mc, P_{1i} = 10.5 WATTS, P_{2i} IS VARIABLE)

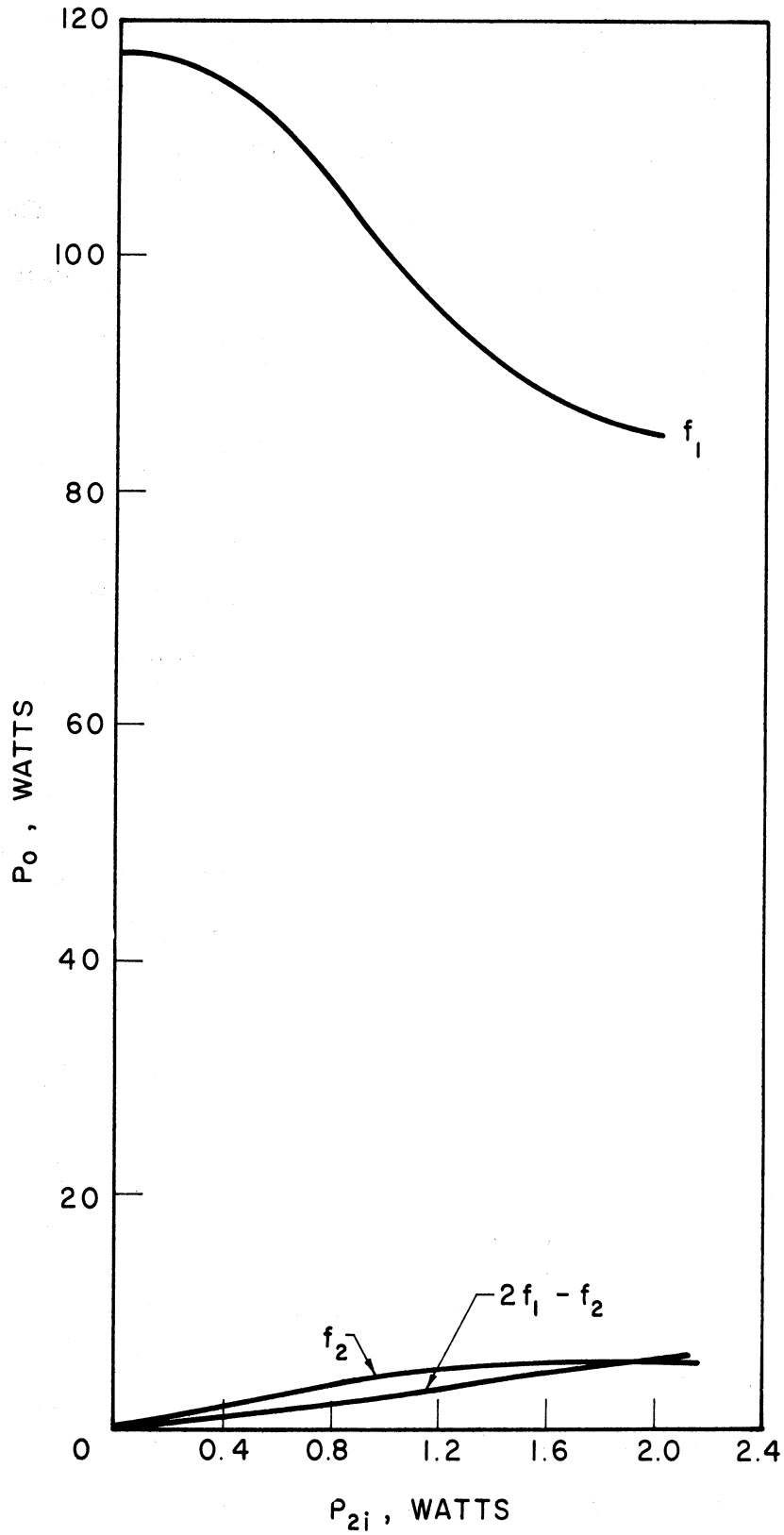

FIG. 5.10 OUTPUT POWERS AS THE f_2 INPUT POWER IS VARIED. (f_1 = 260 mc, f_2 = 280 mc, P_{1i} = 13 WATTS, P_{2i} IS VARIABLE)

If the above experiments are repeated with the larger-power input signal P_{1i} applied at a higher frequency than P_{2i} (i.e., $f_1 > f_2$), similar results are obtained. Figure 5.11 illustrates the results for f_1 = 140 mc, f_2 = 120 mc, P_{1i} = 14 watts and a variable P_{2i}. The cross-modulation term $2f_1-f_2$ grows with P_{2i} while the f_1 and $2f_1$ power output terms decrease as before. The $2f_1-f_2$ power is approximately the same as P_{2O}.

Figure 5.12 indicates the results for f_1 = 240 mc, f_2 = 220 mc and P_{1i} = 11 watts. In this case both of the cross-modulation terms $2f_1-f_2$ and $2f_2-f_1$ are present in the output. Again, P_{1O} decreases as P_{2i} increases, thus indicating a transfer of power from the f_1 signal to the cross-modulation terms.

It is apparent from the data that the strongest cross-modulation term is always $2f_1-f_2$ where P_{1i} is greater than P_{2i}. Thus the larger cross-modulation signal appears below f_1 when f_1 is less than f_2 and appears above f_1 when f_1 is greater than f_2.

Figure 5.13 indicates the results when one signal is applied at f_1 = 130 mc and a second signal is applied at the second-harmonic frequency, $f_2 = 2f_1$ = 260 mc. P_{2i} is fixed at 1.05 watts while P_{1i} is increased up to 6 watts. P_{2O} is constant at low P_{1i} levels and then decreases at higher values. The second-harmonic output P_{2f_1} increases as P_{1i} is increased so that the total output at 260 mc is $P_{2O} + P_{2f_1}$ which has a maximum value of approximately 58 watts at P_{1i} = 3 watts. The combined 260-mc output then decreases with further increases in P_{1i}.

Numerous other operating conditions have been evaluated and the results generally have been the same as those described above. The simultaneous application of two separate signals causes the output power

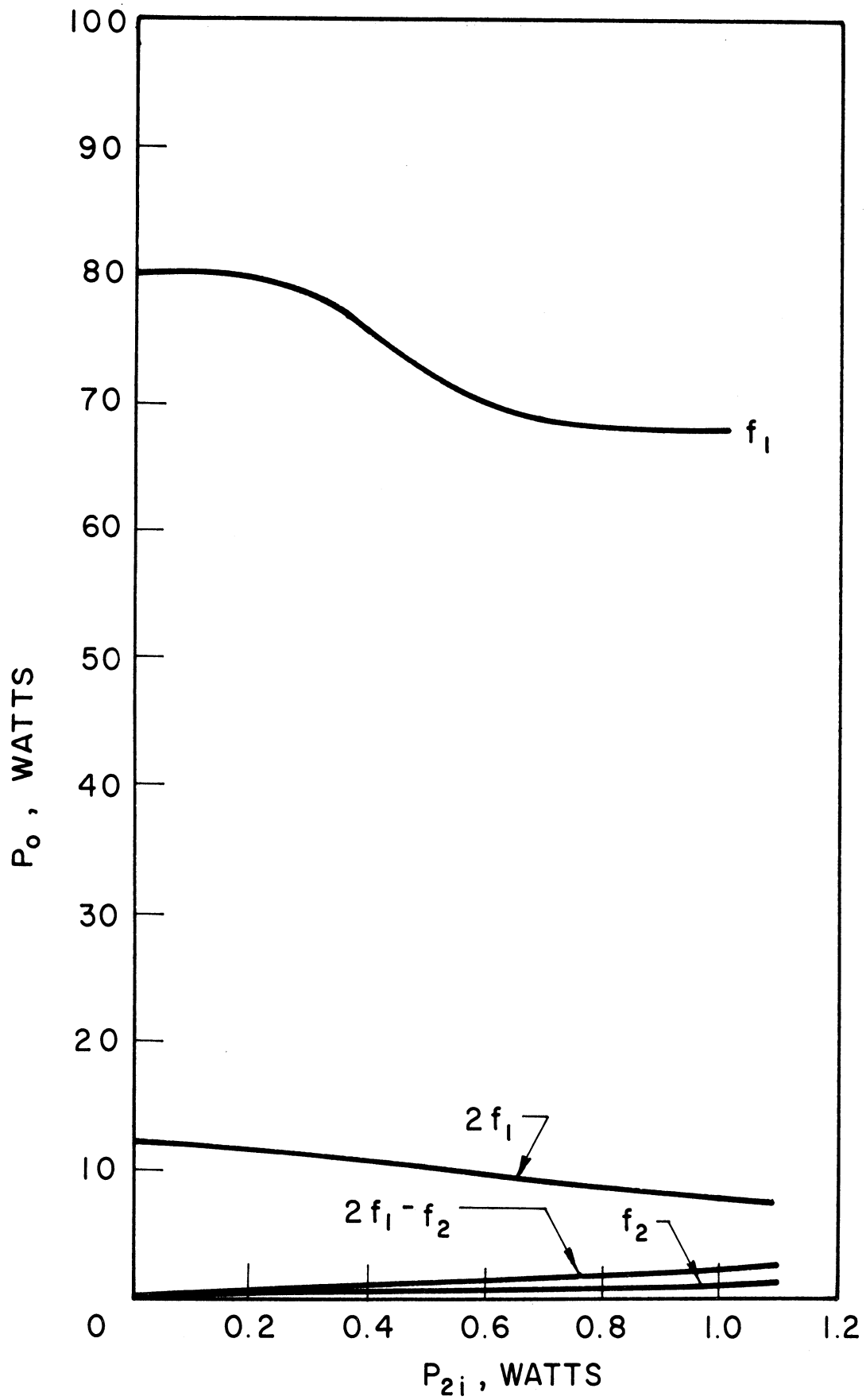

FIG. 5.11 OUTPUT POWERS AS THE f_2 INPUT POWER IS VARIED. (f_1 = 140 mc, f_2 = 120 mc, P_{1i} = 14 WATTS, P_{2i} IS VARIABLE)

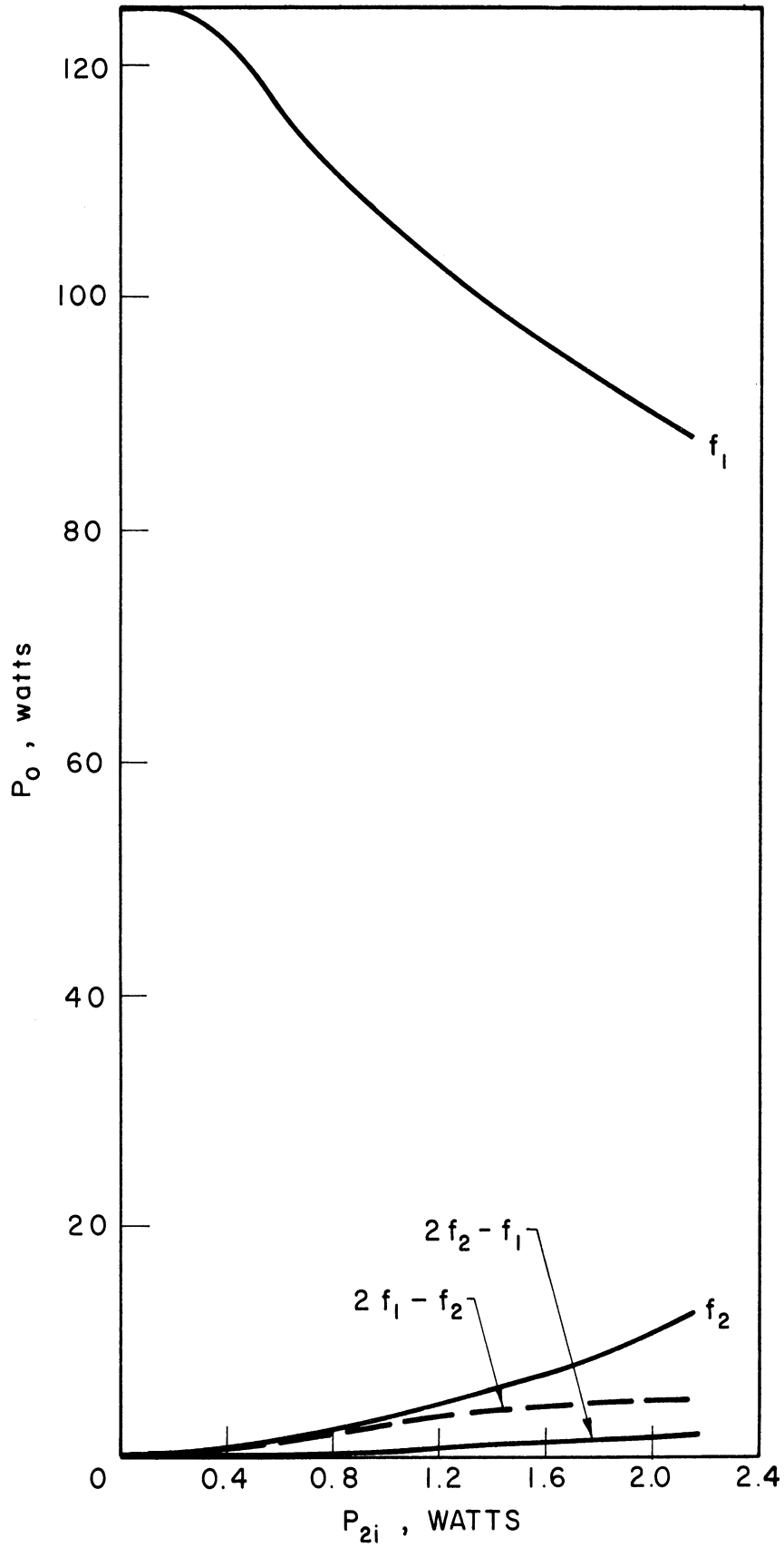

FIG. 5.12 OUTPUT POWERS AS THE f_2 INPUT POWER IS VARIED. (f_1 = 240 mc, f_2 = 220 mc, P_{1i} = 11 WATTS, P_{2i} IS VARIABLE)

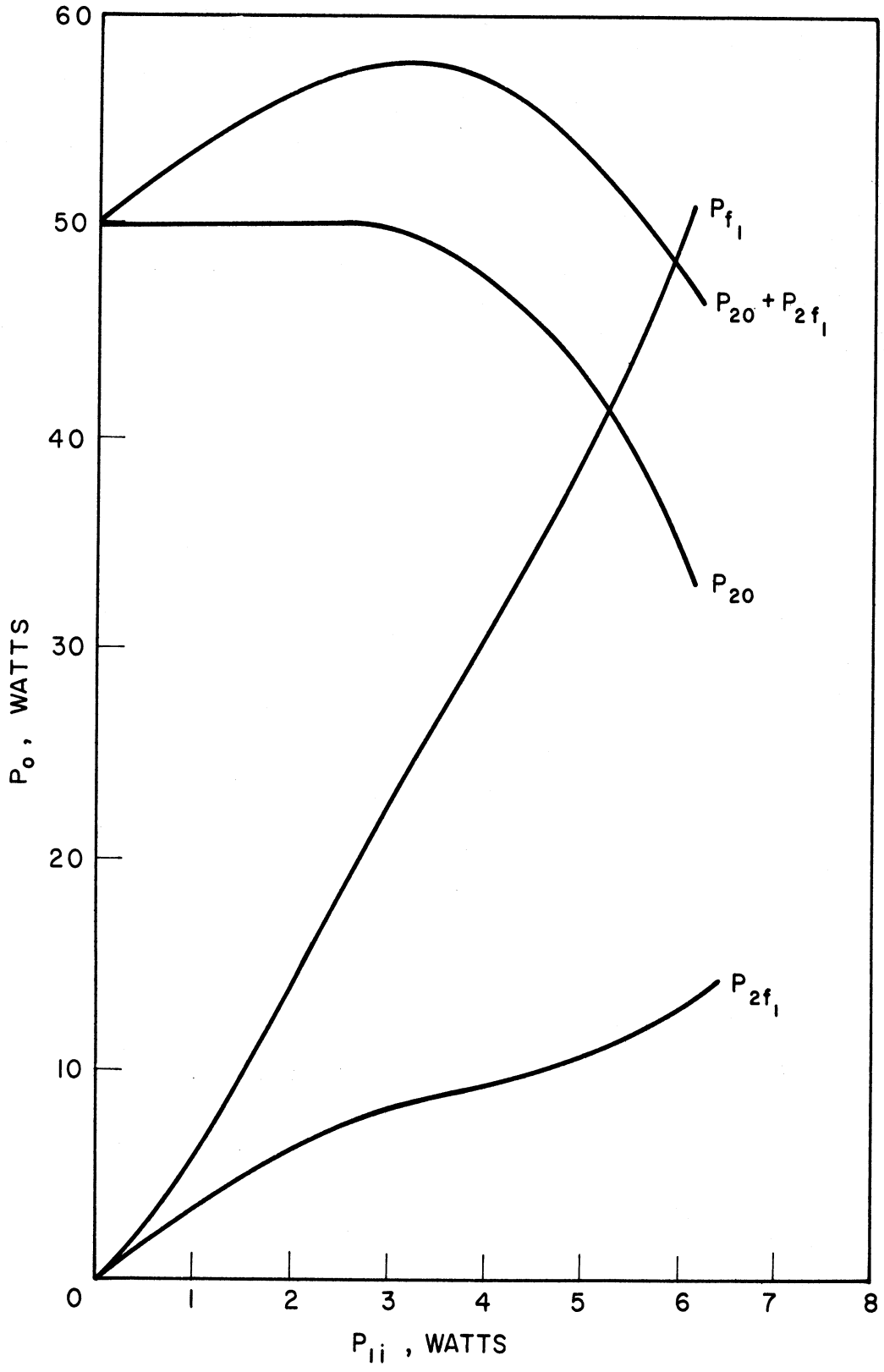

FIG. 5.13 OUTPUT POWERS WHEN SIGNALS ARE APPLIED AT f_1 = 130 mc AND $f_2 = 2f_1$. (P_{1i} IS VARIABLE, P_{2i} = 1.05 WATTS)

of either signal to be less than when only a single frequency is applied. This, of course, is directly a result of the nonlinear nature of the beam-wave interaction process which causes the generation of various cross-modulation terms.

5.4 Conclusions and Program for the Next Quarter. Experimental results have been obtained for the multisignal operation of a Crestatron in the 100-300 mc range. The cross-modulation terms $2f_1-f_2$ and $2f_2-f_1$ occur with increasing amplitudes as the power levels of the input signals are increased. When the two input signals are quite different in power, the larger signal determines the frequency at which the larger cross-modulation term exists; i.e., when P_{1i} is the larger signal, then $2f_1-f_2$ is the larger cross-modulation signal and its frequency is either below or above f_1 depending on whether f_1 is below or above f_2.

The investigations will be continued during the next quarter. Attempts will be made to apply two saturation-level signals to the Crestatron and to observe the various cross-modulation signals which are generated. The possibility of applying a band of noise and a signal frequency is being investigated and it is hoped that such an experiment will be completed during the next quarter. The multisignal operation of a tapered-helix tube will also be investigated to determine the effect of circuit tapering on the generation of cross-modulation signals.

6. Theoretical Studies on Multisignal Microwave Amplifiers

(J. E. Rowe)

6.1 Nonlinear O-Type Amplifier Calculations. In previous calculations[1] on the nonlinear characteristics of O-type traveling-wave

---

1. El-Shandwily, M. E., "Analysis of Multi-Signal Traveling-Wave Amplifier Operation", Tech. Report No. 85, Contract No. NObsr-89274, Electron Physics Laboratory, The University of Michigan; June, 1965.

amplifiers with multisignal r-f inputs, some difficulty was encountered in accurately determining the magnitude of the cross-modulation products. The nonlinear equations adequately describe the multisignal operation and it is felt that the difficulty results from the fact that the magnitudes of the generated signal components near the input are of the same order of magnitude as the error in the numerical procedure and thus the initial growth rates are usually in error. The principal effort during recent months has been directed toward modifying the numerical calculation procedures in order to minimize the error and insure the stability of the system. Specific calculations have been made for a TWA with a single-frequency input and fundamental and second-harmonic outputs. This case was selected because of the availability of a quasi-nonlinear theory to predict the amplitude of the second- and third-harmonic outputs of a nonlinear O-type TWA. These theoretical studies will continue during the next quarter.

6.2 Multisignal Crossed-Field Amplifiers. The small-signal theory of an injected-beam crossed-field amplifier has been generalized to include multisignal inputs as indicated in Quarterly Progress Report No. 8. These equations have recently been programmed for solution on an IBM-7090 digital computer and the program is presently being checked out. It is anticipated that preliminary solutions should be available during the next period. This theory is particularly useful for determining the growth rates of the cross-modulation products and for evaluating the am to pm conversion inherent in multisignal operation of a nonlinear microwave amplifier.

6.3 Nonlinear Theory of Multisignal Crossed-Field Amplifiers. The nonlinear theory of crossed-field injected beam amplifiers with

multisignal inputs can be developed along the same lines as that for the nonlinear O-type amplifier. Further progress on this problem awaits the satisfactory solution of the numerical accuracy and stability problem described in Section 6.1.

6.4 Program for the Next Quarter. Plans for the next quarter include further work on the numerical accuracy and stability problem associated with the nonlinear analysis of the multisignal O-type amplifier and the completion of check runs on the multisignal crossed-field amplifier using a generalized small-signal analysis. It is also anticipated that experimental work can be initiated on the multisignal crossed-field amplifier.

7. General Conclusions (C. Yeh)

Beam expansion in a quadrupole amplifier has been studied by introducing a nonrotating beam of radius ρ_o into a quadrupole structure at the proper d-c potential and by computing the trajectories of the peripheral electrons at different locations in response to the structure field. Both modes of operation, i.e., cyclotron-cyclotron and cyclotron-synchronous wave interactions, have been studied and compared. It can be concluded that the former mode is subject to much less beam expansion than the latter. However, from the actual trajectories of the electrons in cyclotron-synchronous wave interaction, electrons from different entrance angles of the beam are quickly brought into focus with those from the most favorable entrance angle, i.e., they are bunched into a beam for favorable interaction. Therefore the beam expansion due to the pump field action should not present a serious problem.

Theoretical results on the cross-modulation products at the output of a tunnel-diode amplifier due to two input signals of slightly

different frequencies have been computed. For an X-band amplifier in which the second harmonics of the input signals are not inside the bandwidth of the amplifier, the $2f_1-f_2$ and $2f_2-f_1$ products become important. As the ratio of the amplitudes, a_2/a_1, is increased, both of these components increase, one almost linearly ($2f_1-f_2$) and the other almost quadratically ($2f_2-f_1$). If f_1 is the larger signal, then the component $2f_2-f_1$ becomes more important than the component $2f_1-f_2$. Also, the amplitude of the input decreases as a_2/a_1 is increased. These are general phenomena in all nonlinear devices. It is expected that the relative importance of the $2f_2-f_1$ and $2f_1-f_2$ components will change as the bias point and the maximum voltage swing are changed. This effect will be studied in the next quarter.

The Crestatron is a power amplifier operating on the principle of beating-wave amplification. It has been found that the second-harmonic output of this amplifier is quite high over the entire input power range and generally is only 4-5 db below the fundamental output level. With multiple-signal input operation, if second harmonics are not within the operating range of the amplifier, then the important components are again the $2f_1-f_2$ and $2f_2-f_1$ signals. If, however, the power level of f_1 is greater than that of f_2, the important contribution is from the $2f_1-f_2$ component and that from the $2f_2-f_1$ component is negligibly small.

DISTRIBUTION LIST

No. Copies	Agency
3	Chief, Bureau of Ships, Department of the Navy, Washington 25, D. C., Attn: Code 681A1D
1	Chief, Bureau of Ships, Department of the Navy, Washington 25, D. C., Attn: Code 681B2
1	Chief, Bureau of Ships, Department of the Navy, Washington 25, D. C., Attn: Code 687A
3	Chief, Bureau of Ships, Department of the Navy, Washington 25, D. C., Attn: Code 210L
1	Chief, Bureau of Naval Weapons, Department of the Navy, Washington 25, D. C., Attn: Code RAAV-333
1	Chief, Bureau of Naval Weapons, Department of the Navy, Washington 25, D. C., Attn: Code RAAV-61
1	Chief, Bureau of Naval Weapons, Department of the Navy, Washington 25, D. C., Attn: Code RMGA-11
1	Chief, Bureau of Naval Weapons, Department of the Navy, Washington 25, D. C., Attn: Code RMGA-81
1	Director, U. S. Naval Research Laboratory, Washington 25, D. C., Attn: Code 524
2	Director, U. S. Naval Research Laboratory, Washington 25, D. C., Attn: Code 5437
2	Commanding Officer and Director, U. S. Navy Electronics Laboratory, San Diego 52, California, Attn: Code 3260
2	Commander, Aeronautical Systems Division, U. S. Air Force, Wright-Patterson Air Force Base, Ohio, Attn: Code ASRPSV-1
2	Commanding Officer, U. S Army Electronics Research and Development Laboratory, Electron Devices Division, Fort Monmouth, New Jersey
3	Advisory Group on Electron Devices, 346 Broadway, 8th Floor, New York 13, New York
1	Commanding General, Rome Air Development Center, Griffiss Air Force Base, Rome, New York, Attn: RCUIL-2
20	Headquarters, Defense Documentation Center, For Scientific and Technical Information, U. S. Air Force, Cameron Station, Alexandria, Virginia

No. Copies	Agency
1	Microwave Electronics Corporation, 3165 Porter Drive, Stanford Industrial Park, Palo Alto, California
1	Bendix Corporation, Systems Division, 3300 Plymouth Road, Ann Arbor, Michigan, Attn: Technical Library
1	Litton Industries, 960 Industrial Road, San Carlos, California, Attn: Technical Library
1	Dr. R. P. Wadhwa, Electron Tube Division, Litton Industries, 960 Industrial Way, San Carlos, California
1	Microwave Associates, Burlington, Massachusetts, Attn: Technical Library
1	Microwave Electronic Tube Company, Inc., Salem, Massachusetts, Attn: Technical Library
1	Radio Corporation of America, Power Tube Division, Harrison, New Jersey
1	Raytheon Company, Burlington, Massachusetts, Attn: Technical Library
1	S-F-D Laboratories 800 Rahway Avenue, Union, New Jersey, Attn: Technical Library
1	Westinghouse Electric Corporation, P. O. Box 284, Elmira, New York, Attn: Technical Library
1	Mr. A. Weglein, Hughes Aircraft Company, Microwave Tube Division, 11105 South LaCienaga Boulevard, Los Angeles 9, California
1	The University of Arizona, University Library, Tucson, Arizona
1	Eitel-McCullough, Inc., 13259 Sherman Way, North Hollywood, California, Attn: Dr. John E. Nevins, Jr.
1	Hughes Aircraft Company, Microwave Tube Division, 11105 South LaCienaga Boulevard, Los Angeles 45, California 90009, Attn: Dr. John Mendell